HEAT TRANSFER AUGMENTATION IN A DE-SUPERHEATER OF DOMESTIC REFRIGERATOR WITH TWISTED TAPE TURBULATORS

A

THESIS

Submitted in fulfillment of the requirements for the award of

Master of Engineering (M.E.)

In

Thermal Engineering

Submitted by

Akshay Bhardwaj

(ROLL NO. 801683004)

UNDER THE GUIDANCE OF

Faculty Supervisor

Dr. Rohit Kumar Singla

Assistant Professor (MED)

Industrial Supervisor

Dr. Prasanth Anand Kumar Lam

Assistant Manager (LG Soft PVT.LTD.)

DEPARTMENT OF MECHANICAL ENGINEERING

THAPAR INSTITUTE OF ENGINEERING AND TECHNOLOGY, PATIALA-147004

JULY, 2018

CERTIFICATION

I, Akshay Bhardwaj, declare that this thesis report entitled "***Heat transfer augmentation in a de-super-heater of domestic refrigerator with twisted tape turbulators***", submitted towards fulfillment of the requirements for the award of Master's Degree in Thermal Engineering, in Mechanical Engineering Department of Thapar Institute of Engineering and Technology, Patiala is entirely my own work during the six months internship at LG Soft PVT. LTD. from January to July, 2018. This document has not been submitted for any degree in any other institution.

Akshay

Date: 30th July, 2018 — **Akshay Bhardwaj**

Place: TIET, Patiala — 801683004

Thapar Institute of Engineering and Technology, Patiala

This is to certify that above statement made by the candidate is correct and true to the best of my knowledge.

Dr. Rohit Kumar Singla
Assistant Professor, MED
TIET, Patiala
Faculty Coordinator

Dr. Prasanth Anand Kumar Lam
Assistant Manager
LG Soft India PVT. LTD.
Industrial Coordinator

ACKNOWLEDGEMENT

The internship opportunity I had with LG Soft India Private Limited was a great chance for learning and professional development only thanks to Mr. Vikas Bakshi, Assistant General Manager of LG Soft India Private Limited for providing me this golden opportunity. Therefore, I consider myself as a very lucky individual as I was provided with an opportunity to be a part of it. I am also grateful for having a chance to meet so many wonderful people and professionals who led me though this internship period.

Bearing in mind, I am taking this opportunity to express my deepest gratitude and special thanks to the Late Mr. N.K. Jain, Director of LG Soft India Private Limited in spite of being extraordinarily busy with his duties, took time out to hear, guide and keep me on the correct path and allowing me to carry out my project at their esteemed organization.

I express my deepest thanks to Mr. Brijesh Sharma, Deputy General Manager for taking part in useful decision & giving necessary advices and guidance and arranged all facilities to make work easier. I choose this moment to acknowledge his contribution gratefully.

It is my radiant sentiment to place on record my best regards, deepest sense of gratitude to Dr. Prasanth Anand Kumar Lam, Assistant Manager and Dr. Rohit Kumar Singla, Assistant Professor (MED), for their careful and precious guidance which were extremely valuable for my study both theoretically and practically.

I perceive this opportunity as a big milestone in my career development. I will strive to use gained skills and knowledge in the best possible way, and I will continue to work on their improvement, in order to attain desired career objectives. Hope to continue cooperation with all of you in the future.

Akshay Bhardwaj

801683004

ABSTRACT

In domestic refrigerator, De-Super-heater which is also called as Pipe Joint Assembly (PJA), is a serpentine tube which is immersed in tray-drip and connecting compressor outlet and condenser inlet. It is used to desuperheat the super heated refrigerant vapor coming out from the compressor and also used to evaporate the defrost water in the tray drip. The computational fluid dynamics analysis was done by using commercial CFD (Computational Fluid Dynamics) algorithm, ANSYS FLUENT on PJA and obtained results were compared with the analytical as well as experimental results. In the present study, the effect of turbulators on heat transfer augmentation in PJA is simulated with different mass flow rates. Also, a parametric study was performed to estimate the effect of PJA tube diameter and PJA length by keeping the surface area constant and insert the twisted tape of different twist ratios and clearance ratios inside the tube. Pressure drop and heat transfer behavior in a twisted tape swirl generator inserted tube are investigated numerically. The twisted tapes are inserted inside the tube separately from the tube wall. The effect of different twist ratios (y/D = 5, 6 and 7) and the clearance ratios (c/D = 0.166, 0.272 and 0.4) are discussed for the different mass flow rates ($\dot{m}$ = XX,XX and XX gm/s). Calculated transfer coefficient and the temperature of stagnant water are applied to the external surface of the tube wall. The iso-butane refrigerant is selected as working fluid. The obtained results from the plain tube are validated by well known equations given in the literature. With increase in the diameter of the tube from XX mm to XX mm and decrease the length of the tube from XX mm to XX mm in order to keep the surface area same i.e. XX m^2, the pressure drop reduces from XX Pa to XX Pa and outlet temperature of refrigerant vapor and the total heat transfer rate remains same. The maximum increase of 26% has been obtained in the total heat transfer rate dissipated, whereas an increase of 58% is observed in the pressure drop, when the mass flow rate was increased from XX gm/s to XX gm/s at the inlet of the tube of XX mm diameter. The using of twisted tapes inside the tubes considerably increases the heat transfer rate and pressure drop when compared with the plain tube. The heat transfer rate and the pressure drop are increases with the decreases of clearance ratio (c/D) and twist ratio (y/D), also increase of mass flow rate. As we increase the twist ratio of the twisted tape from 5 to 7 by keeping the same clearance ratio of 0.166, the heat transfer rate decreases from XX Watt to XX Watt and the pressure drop decreases from XX Pa to XX Pa. As we increase the clearance ratio of the twisted tape from 0.166 to 0.4 by keeping the same twist ratio of 5, the heat transfer rate decreases from XX Watt to XX Watt and the pressure drop decreases from XX Pa to XX Pa. The highest heat transfer

enhancement is achieved as 1.32 for c/D = 0.166 and y/D = 5 at mass flow rate of XX gm/s. An increase of 32% is observed in the heat transfer rate and decrease of pressure drop from XX Pa to XX Pa is observed with proposed design in comparison to the actual design.

TABLE OF CONTENTS

Page No.

LIST OF FIGURES

Page No.

LIST OF TABLES

Page No.

NOMENCLATURE

A_c: Cross-sectional Area [m^2]

C_1: Constant

C_2: Constant

D_1: Inner Tube Diameter[m]

D_2: Outer Tube Diameter[m]

D_h: Hydraulic Diameter[m]

L: Length of Tube[m]

L_h: Hydrodynamic Entry Length[m]

L_t: Thermal Entry Length[m]

Nu: Average Nusselt Number

Pr: Prandtl Number

Pr_s: Prandtl corresponding to surface temperature

Re: Reynolds Number

T_b: Bulk Mean Temperature[K]

T_e: Average Temperature at exit of pipe[K]

T_i: Average Temperature at entry of pipe[K]

h: Average Convective heat transfer coefficient[W/m^2K]

$\dot{m}$: Refrigerant Mass Flow Rate [kg/s]

k: Thermal Conductivity [W/mK]

m: Constant

n: Constant

p: Perimeter of Tube [m]

v: Velocity of Fluid [m/s]

ρ: Density of Fluid [kg/m3]

Δp: Pressure Drop [Pa]

χ: Correction Factor

y: Half of pitch [m]

Q: Total Heat Transfer Rate [W]

c: Clearance

D: Width of the Twisted Tape [m]

XX: Confidential Values

Chapter 1 : INTRODUCTION AND OBJECTIVES

1.1 Introduction of Heat Exchanger

Heat exchanger is equipment used to exchange the warm vitality involving atleast two fluids, among the firm particulates and flowing, or among a firm surface and the flowing. Heat exchanger devices are widely used equipments in numerous areas of fields such as chemical engineering, refrigeration and air heating and cooling, petroleum, cryogenic warmth recuperation, elective fuel, fabricating ventures, metallurgy and electric power; they are also a very important component of many industrial products available in the market. Great warmth exchange execution is very critical and pivotal for the warmth exchangers because it is straigth forwardly identified with the vitality sparing advantages. The warmth exchangers can be arranged from multiple point of view, for example, as indicated by quantity of fluids and warmth exchange instrument. Ordinary warmth exchangers are ordered based on the flow arrangement and the construction type. The other strategy used to order the warmth interchangers are sort of procedure capacities and the type of fluids included such as gas- gas, gas-liquid, liquid-liquid and two stage gas. Another important arrangement of heat exchanger according to the surface compactness named as compact heat exchangers. Another essential order of the warmth exchanger as indicated by the surface conservativeness named as reduced warmth interchangers.

A gas-to-liquid warmth interchanger is alluded to as conserative warmth interchanger if the surface zone thickness of the warmth exchange surface is more prominent than 700 m^2/m^3or hydraulic diameter is less than 6 mm for working in a gas stream and 400 m^2/m^3or superior for working in fluid. The warmth exchanger is alluded as meso warm exchanger if its surface thickness is more noteworthy than 3000 m^2/m^3or hydraulic diameter is in middle of 100 µm to 1 mm and warmth exchanger is alluded as small scale warm interchanger if its shell zone thickness is more prominent than 15,000 $m^2/m^3$and its hydraulic diameter is in the middle of 1 µm to 100 µm. A shell and tube warm exchanger has a surface territory thickness under 100 $m^2/m^3$with plain tubes on one fluid side. A gas-to-liquid warmth interchanger is alluded to as conserative warmth interchanger if the surface zone thickness of the warmth exchange surface is more prominent than 700 m^2/m^3or hydraulic diameter is less than 6 mm for working in a gas stream and 400 m^2/m^3or superior for working in fluid.

1.2 Extended Surface Heat Exchangers

Based on constructional point of interest, heat exchangers may be characterized keen on Plate into Plate-type, tubular, regenerative compose heat exchangers and the broaden surface. For the adequancy underneath the 60%, the tubular and plate-type exchangers are principally utilized in a large portion of the cases and the surface region thickness of these heat exchangers is under 700 m^2/m^3. To have blades (extended suraface) is a standout amongst the most widely recognized strategies to build the minimization and the surface region. The surface zone can be expands 5 to 12 times the essential zone with the expansion of balances.

1.2.1 Plate Fin Heat Exchanger

In this type of heat exchangers fins triangular or rectangular cross-sections are sandwiched between the parallel plates as shown in Figure 1.1.

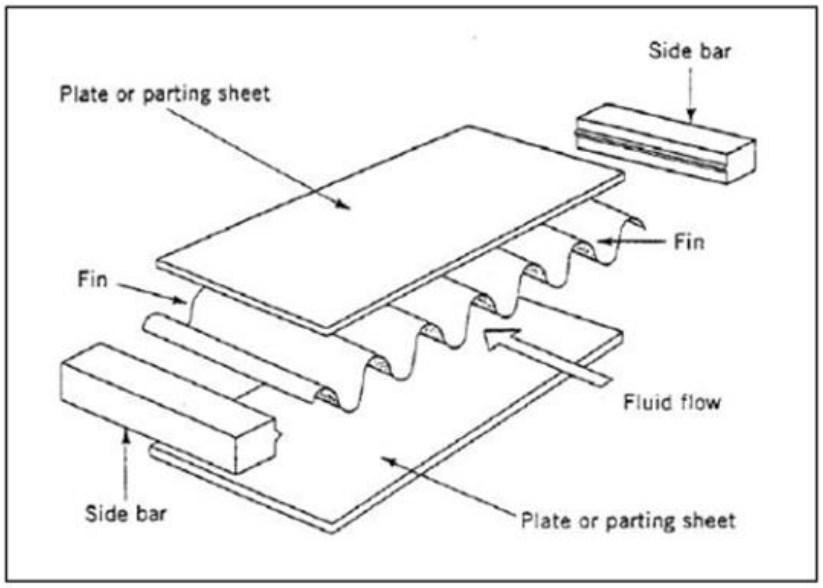

Figure 1.1 : Basic component of plate-fin heat exchanger

Fins are formed with bite the dust are connected with the plates by patching, cement holding, expulsion and mechanical fit.

Plate-blades are classified as: 1) Plain fins 2) Plain yet wavy fins, and 3) interfered with balances. Figure 1.2 demonstrates a portion of the blades which are most usually utilized in warm interchanger. The balances and plates are prepared of an assortment of resources.They are broadly utilized in power plants, refrigeration, water pump, warm pump,

cryogenic, aerating and cooling, squander warm recuperation and gas-liquefaction.

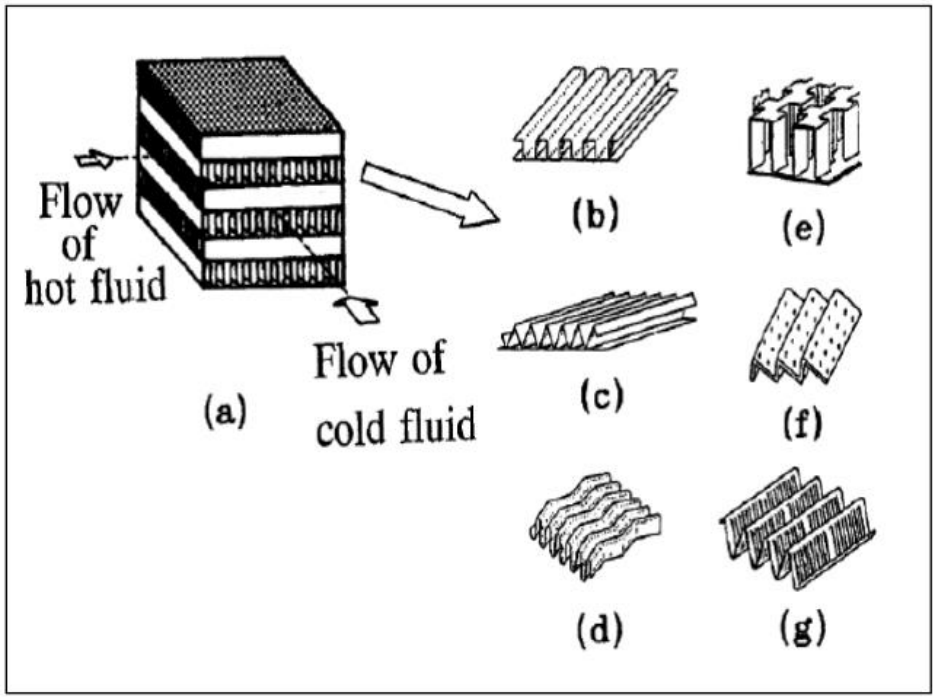

Figure 1.2: Plate-fin heat exchanger and its geometries

1.2.2 Tube Fin Heat Exchanger

The tube-fin warm exchangers are additionally named 1) customary and 2) particular tube-balance exchangers. In tube-fin warm exchanger, warm exchange happens through the tube surface by conduction. In tube-balance exchanger, rectangular, round and circular tubes are utilized. Blades are utilized outside the tube; be that as it may, balances might be utilized within the tubes too, if required as appeared in Figure 1.3.

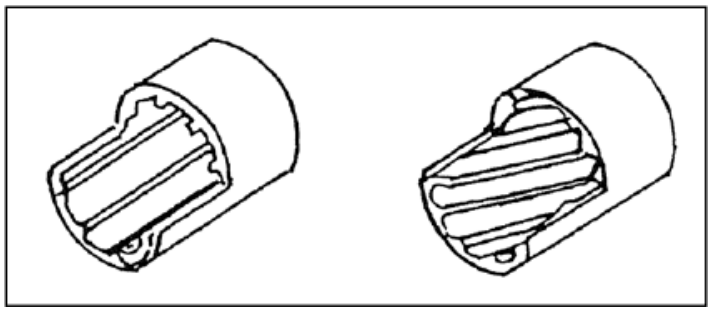

Figure 1.3: Internally finned tubes

Contingent upon the balance compose, these warmth exchangers can be additionally named a) persistently finned tube, b) separately finned tube and c) longitudinally finned warm interchangers. Figure 1.4 demonstrates the two fundamental sorts of tube-blade warm interchangers. For the consolidating applications longitudinal balances are by and large utilized.

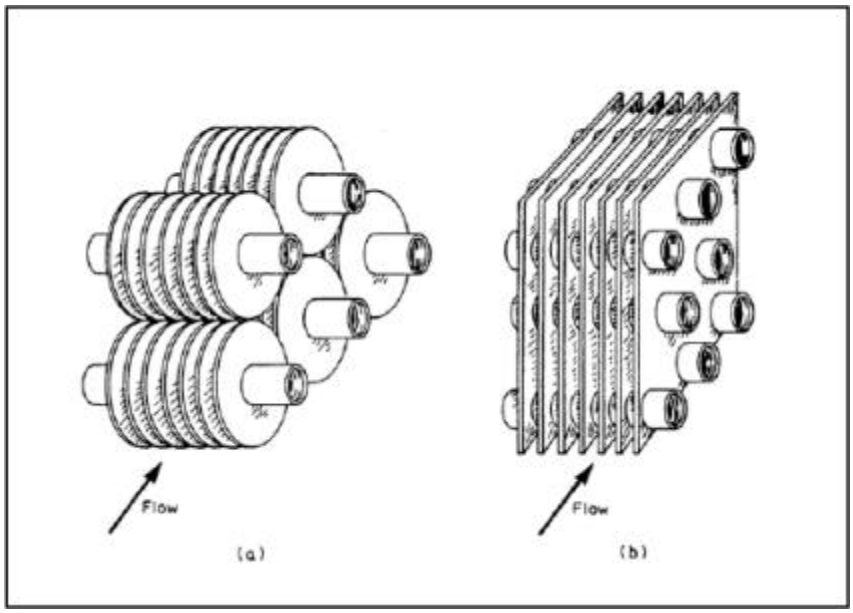

Figure 1.4: Externally Finned Tubes

1.3 Other Heat Transfer Augmentation Methods

Around 14 warm exchange upgrade procedures are recognized by Bergles et al. [1983] can be utilized for the warmth exchangers. Proposals warm exchange upgrade methods for the most part ordered into dynamic and uninvolved procedures. Uninvolved method don't require any outer power contribution to expand the warmth exchange rate; rather they utilize it from the framework itself which prompts increment in liquid weight drop, while the dynamic strategies requires outside power contribution to cause the coveted stream alteration and change in the rate of warmth exchange.

1.3.1 Active Heat Transfer Enhancement Methods

These strategies are extremely mind boggling from the utilization and configuration perspective as the strategy requires outer power contribution to cause the coveted stream alteration and change in the rate of warmth exchange e.g. Mechanical guides, surface vibration, liquid vibration, electrostatic field, infusion, suction and stream impingement. Since, of these need of outside power in numerous viable applications it discovers restricted applications.

(a) Motorized Guides

These guides comprise of pivoting the surfaces or blending the liquid by mechanical means. For the upgrade of warmth exchange mechanical surface scrapper might be connected to the

channels of the gases. To expand the warmth exchange turning heat exchanger channels are monetarily utilized.

(b) Surface Vibration

For the single stage warm exchange growth high or low recurrence surface vibrations are utilized. To vibrate a warmth exchange surface a piezoelectric gadget may likewise be utilized. To pulsate plate at around 2.5 kHz Heffington et al. utilizes a piezoelectric transducer, which delivers a shower of the little distance across drops on the bubbling surface.

(c) Fluid Vibration

Because of the mass of the warmth exchangers the liquid vibration is the pragmatic sort of vibration improvement. From throb the liquid vibrations scope of around 1 Hz ultrasound and connected for single stage liquids.

(d) Electrostatic Fields

Electrostatic field delivered by moreover substituting present is utilized for dielectric liquids to effect legitimate mass blending of liquid in region of warmth area exchange facade. The electric meadow connected to dielectric liquid forces cadaver drive on liquid which impacts smooth movement. Yabe [1991] gave a fantastic depiction of the basics of EHD improvement.

(e) Infusion

Now the gas is provided to stream of fluid in the course of the permeable facade or a similar liquid is infused upstream. The infused gas increases the solitary stage stream.

(f) Suction

Suction includes the procedure of vapor evacuation liquid withdrawal through a permeable warmed facade. This procedure is connected to just single stage liquids.

(g) Stream impingement

Stream impingement includes splashing fluid on warm facade which spreads as emaciated layer and gets dissipated. For this reason, different planes might be utilized. Splash cooling particularly includes impinging fluid as little beads. Pais et al. [1992] and Xia [2002] have dealt with the water impingement.

1.3.2 Passive Heat Transfer Enhancement Techniques

These techniques don't require any outside power contribution to expand the heat exchange rate; rather they utilize it from the framework itself which prompts increment in fluid pressure drop. They for the most part utilize geometrical changes to stream conduit utilize embeds, for illustration, twisted tape (convoluted tape), surface covering, wavy surfaces, swirl devices, harsh surfaces and expanded surface development. They increment the heat transfer coefficient by exasperating or changing the current stream conduct.

(a) Coating of the Surfaces

Condensation happens at first glance whose temperature is not as much as the vapor immersion temperature. This condensed fluid at first glance exists in beads. Drop savvy buildup yields high heat transfer coefficient yet it can't be maintained for all time. Non-wetting covering, for example, Teflon, upgrade the drop-wise condensation. A hydrophilic coating advances the condensate seepage on evaporator balances by decreasing the wet pneumatic force drop. A permeable covering on base surface is a powerful upgrade strategy for film condensation. Condensate seepage is helped by narrow stream inside the permeable covering, bringing about a diminishing of the condensate film thickness.

(b) Extended Surfaces

It is a most regular way to deal with upgrade the warmth exchange by utilizing the expanded surfaces. The expanded surfaces for fluids normally utilize considerably littler balance statures than utilized for fluids due to the privileged warmth exchange coefficient for fluids. Utilization of lofty balances with fluids would consequence in stumpy balance effectiveness and result in poor material usage. It is a most regular way to deal with upgrade the warmth exchange by utilizing the expanded surfaces. The expanded surfaces for fluids normally utilize considerably littler balance statures than utilized for fluids due to the superior warmth exchange coefficient for fluids. The expanded surfaces for fluids normally utilize considerably littler balance statures than utilized for fluids due to the superior warmth exchange coefficient for fluids. It is a most general approach to manage redesign the glow trade by using the extended surfaces. The extended surfaces for liquids regularly use impressively more diminutive adjust statures than used for liquids because of the prevalent warmth trade coefficient for liquids. The extended surfaces for liquids regularly use significantly smaller adjust statures than used for liquids because of the prevalent warmth trade coefficient for liquids.

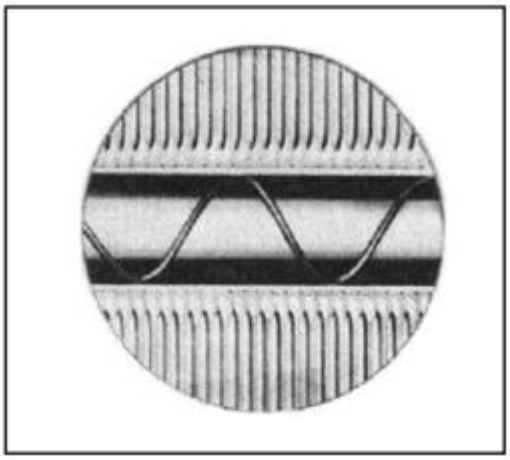

Figure 1.5: Wire coil inserts

(c) Displaced inserts

These are campaign embedded into stream conduit to enhance vitality convey at warmed facade in a roundabout way. The dislodged embeds blend the primary stream notwithstanding that in the divider locale. Dislodged wire curl embed (Figure 1.6) isn't connected to mass of tube. These devices intermittently blend gross stream arrangement however not influencing primary stream essentially. The dislodged embeds blend the primary stream notwithstanding that in the divider locale. Dislodged wire curl embed isn't connected to the mass of the tube.

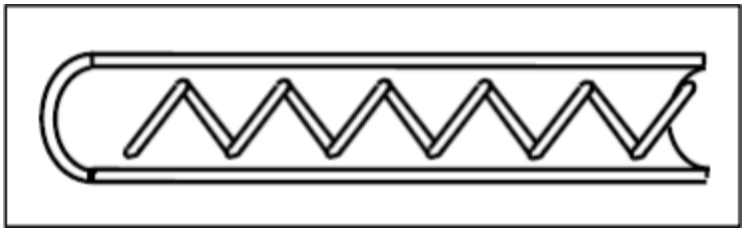

Figure 1.6: Displaced wire coil inserts

(d) Swirl flow devices

These devices incorporate various geometrical game plans or tube embeds for constrained stream that make pivoting or optional stream. Full length contorted tape embeds and pivotal loop embeds with fasten compose meandering are a few cases of churn stream devices. These devices intermittently blend gross stream arrangement however not influencing primary stream essentially. The dislodged embeds blend the primary stream notwithstanding that in the divider locale.

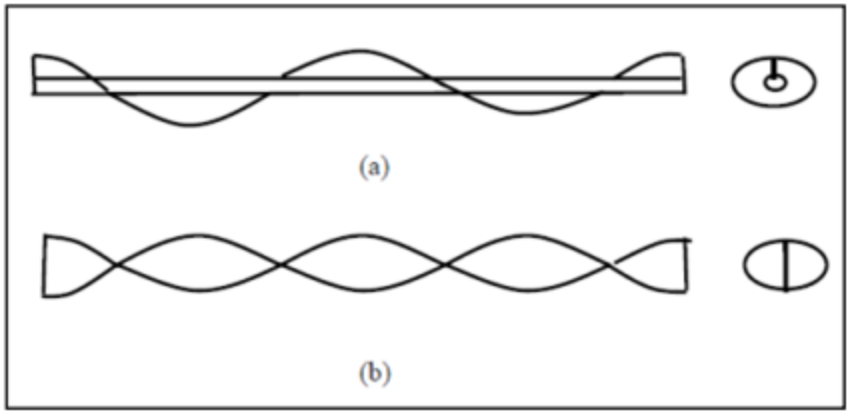

Figure 1.7: Swirl flow devices

Twisted tape swirl turbulator is widely used reflexive types for the heat relocate enhancement due to, ease of installation and simple configurations. Twisted tapes are formed with the aluminium tape by twisting with the mechanical means and these twisted tape type turbulator produce swirling streams and cause enhance fluid amalgamation between nearly wall province and central province at expense of an increased pressure drop so, the heat relocate in tubes can be improved by fluid amalgamation without the need of any outside power source. As a result of its ease and simplicity of assembling establishment, the twisted tape turbulators has been utilized to deliver compact heat exchangers and to build the heat execution of the current heat exchanger. The most surely understood twisted tape configuration is full length twisted tape whose length is equivalent to that of the direct in which it is embedded. Subsequently, the present numeric numerical analysis has been completed to contemplate the pressure, temperature and velocity distribution of the refrigerant vapor goes through the pipe joint assembly with and without twisted tape turbulators of various twist ratios (y/D = 5, 6 and 7) and clearance ratios (c/D = 0.166, 0.272 and 0.4) at distinctive mass stream rates ($\dot{m}$ = XX gm/s, XX gm/s and XX gm/s) utilizing commercial code, Fluent. The CFD results approved with the experimental outcomes and ansys results.

1.4 Objectives

The following objectives have been undertaken in the present study:

1. To contemplate the impact of varying Reynolds number on heat relocate augmentation and pressure plummet for all the designs of PJA.
2. To simulate the actual design of pipe joint assembly using commercial CFD (Computational Fluid Dynamics) algorithm, ANSYS FLUENT and to obtain the temperature as well as

pressure distribution for the same.

3. To perform the simulation by changing the geometrical and flow parameters of the pipe joint assembly to maximize the heat relocate augmentation and minimize the pressure drop.

4. To simulate impact of Twisted tape turbulator of various twist and clearance ratios inside tube and compares it with the consequences of plain tube.

5. Validate the CFD results with the experiment results as well as analytical results.

Chapter 2 : LITERATURE REVIEW

The literature based on the previous research work carried out on the design, analysis and optimization of tube with twisted tape turbulators has been studied and presented in the following text.

V. Hejari and A. Afshari [1] have contemplated the impact of wound tape embeds on the heat exchange and pressure drop change. They perform investigates a unadorned tube and four dissimilar tubes with twist ratios of 6,9,12 and 15. It is establish from outcomes that twisted tape with twist ratio 6 gives the most elevated improvement in warmth exchange coefficient and greatest pressure drop contrasted with simple tube. The upgrade in warm exchange and pressure drop is expanded by 40% and 240% in examination with to the plain tube. It is seen from outcomes that contorted tape with bend ratio of 9 has preeminent execution upgrading warmth exchange with least pressure drop.

B. Halit *et al.* [2] have considered the impact of various freedom proportions and distinctive curve proportion of the wound tape on the warmth exchange and pressure drop inside tube. The air is chosen as running liquid. The contorted tapes are embedded independently from the tube divider and the impact of curve proportions (y/D = 2, 2.5, 3, 3.5 and 4) and clearance proportions (c/D = 0.0178 and 0.0357) are talked about in scope of Reynolds number from 5132 to 24,989 and commonplace one with c/D = 0 are likewise tried for examination. They connected unvarying warmth motion on the outside surface of the tube divider. Analysis demonstrates that the bend proportion (y/D) has significant impact when contrasted and the clearance proportion (c/D) on warm move in contorted tape embedded tube. The most astounding warmth exchange improvement are gotten as 1.756 for leeway proportion (c/D) = 0.0178 and for the clearance proportion (c/D) = 0.0357 the warmth exchange enhancement is gotten as 1.744. For the turned tape of zero leeway proportion and at contort proportion (y/D) = 2 we get greatest improvement in warm exchange as 1.789. Warmth exchange upgrades is superior in tube with bent tape embedded which has freedom proportion (c/D) = 0.0178 than leeway proportion (c/D) = 0.0357 for all cases. Exploratory outcomes demonstrate that utilizing contorted tape independently from tube divider rather than connected sort can likewise supply the improvement in warm exchange and furthermore furnish less tainting when contrasted and the appended one.

E. Smith et al. [3] have examined the impact of length proportion of the short length contorted

tape mounted at the passage test segment. They examined on the short curved tape of length proportion 0.29, 0.43, 0.57 and 1 with just single contort proportion estimation of 4. The diminutive piece tape is utilized as whirling stream gadget for producing solid twirl stream at the tube passage before rotting along the tube. They demonstrate the variety of warmth exchange and weight misfortune as Nusselt number and rubbing factor. The Nusselt number estimations of diminutive piece contorted tape with length proportion equivalents to 0.29, 0.43 and 0.57 are 1.16, 1.22 and 1.27 times the simple tube individually and the estimation of grating component at three distinctive length proportions are 1.76, 1.88 and 1.99 separately. The Nusselt number and grating variable estimations of the short bent tape embed with length proportion (LR) of 0.29, 0.43 and 0.57 separately are around 14%, 9.5% and 6.7%; and 21%, 15.3% and 10.5% lower than that of full length tape. The most extreme improvement efficiencies of diminutive piece contorted tapes are around 0.95, 0.98 and 1.00 for LR= 0.29, 0.43 and 0.57 separately. They likewise frame relationships for Nusselt number and contact aspect adjacent to tape-length proportions and Reynolds number and that connections are approved with trial information with ± 7% digression for both Nusselt number and rubbing factor values.

E. Smith et al. [4] have contemplated trial examination of warmth exchange and stream contact in roundabout tube fixed with consistently divided wound strip components. The inward and external tube measurements are taken as 50.6 and 25.8 mm separately. Chilly and heated water were utilized as running liquids in shell and tube side. They take turned tapes which are made of hardened steel bit with thinness of 1 mm and piece of 1500 mm. They embedded FLTT at various contort proportions (y/D=6 and y/D= 8) and with different leeway proportions (c/D= 1, 2 and 3). They compared the outcomes got from the tube with the bent tape embeds with the tube without the curved tape. They found that by embeddings the diverse sorts of curved tape inside the tube enhance the warmth exchange rate proficiently yet the rubbing element of the tube with bent tape embeds alsoincreases. They additionally contemplated the impact of curve proportion of bent tape on the warmth exchange rate. They found that the mean Nusselt numbers for the bend proportion y = 6 and y = 8 are 179% and 143% separately, superior to anything the plain tube and the grinding factor for the tube with wind proportion y=6 is more than contrast with the tube with contort proportion y = 8. They likewise examined the impact space proportion of contorted tape on the warmth exchange rate. They found that space proportion of S=1 yields the higher estimation of warmth exchange than the more noteworthy space proportion i.e. S=2 and S=3. With the space proportion S=1, S=2 and S=3, the decrease in erosion factor are observed to be around 15%, 39% and 81% separately, in examination with full piece contorted tape.

H.Yen et al. [5] have considered and research tentatively the warmth exchange and grating element attributes of a tube fitted with cross empty bent tape supplements of empty width of 6, 8 and 10 mm under uniform warmth motion. The tube with cross empty wound tape has better warmth exchange improvement under laminar stream than fierce stream. Results demonstrate that Nusselt number and rubbing dynamic diminish as empty width increments from 6 mm to 10 mm. As contrast with simple tube the Nusselt number and rubbing factor for 6 mm empty width increment by 93% to 120% and 883% to 1042% individually. The warmth exchange coefficient and contact factor achieves their most extreme qualities with contorted tape with 6 mm empty width under the fierce stream conditions and the erosion factor and the warmth exchange coefficient achieves their base qualities with wound tape with 8 mm empty width under the violent stream conditions. For decreasing the extra weight drop caused by the supplements the empty part is a practical structure and supportive as far as vitality sparing.

N. Piriyarungrod et al. [6] have contemplated the impact of numerous bent tape (M-TT) at various tape numbers (N = 2,3,4,5 and 6) and bend proportion (y/D = 2.5,5,10,15,20 and 25) on rubbing factor, warm exchange upgrade and thermo-water powered execution practices. As contrast with the single curved tape the utilization of multi-bent tape (M-TT) expands the warmth exchange significantly and contact factor additionally increment because of the vortex impacts and multi-whirling streams. The Nusselt number and contact factor increment with diminishing turn proportion and with expanding tape number for numerous contorted tapes. At tape number (N) = 6 and turn proportion (y/w) = 2.5 most extreme warmth exchange rate and grinding factor acquired at Re = 20,000. The highest thermo- hydraulic recital aspect of 1.2 is obtained by use of multi-twisted tape with tape number (N) = 6 and twist ratio (y/w) = 2.5.

E. Smith et al. [7] have examined the impact of two sorts of bent tapes on the warmth exchange rate and the contact factor. They take run of the mill contorted tape and exchange clockwise and counterclockwise bent tapes for consider. They tried the nine distinctive counter clockwise contorted tape with three diverse curve proportions (y/D) of 3, 4 and 5 each with three bend edges (Θ) = 30^o, 60^o and 90^o. They utilized the water as working liquid and played out the analysis over scope of Reynolds number of 3,000 to 27,000 under uniform warmth motion conditions. The acquired outcomes demonstrate that counter clockwise contorted tape gives higher warmth exchange and grinding factor when contrasted with regularly bent tape at the same working conditions. The outcomes additionally demonstrate that with the expansion of contort edge esteems and with the diminishing of wind proportion, the warmth exchange rate of

counter clockwise bent tape increments. Nusselt quantities of the tube fitted with counter clockwise turned tapes are higher than the Nusselt quantities of the tube fitted with the regular curved tape around 12.8 - 41.9% for various scope of Reynolds number, wind proportion and bend edge.

L. Pengxiao et al. [8] have mimicked the impact of midway empty thin bent tape and its impact on the warmth exchange upgrade execution of a tube under laminar stream conditions. They utilized business CFD programming FLUENT 6.3 which depends on the limited volume strategy and they utilized SIMPLE calculation for finding the answer for the coupling amongst weight and speed. They utilized tetrahedral network for cross section the model and framework close to the divider limit is profoundly refined. The outcomes demonstrate that the tube with cross empty wound tape indicates great by and large execution and the littler leeway is better for warm exchange upgrade.

P. Bharadwaj et al. [9] have contemplated the impact of spirally furrowed tube with and without the bent tape on the improvement of warmth exchange rate and the weight drop over the extensive variety of the Reynolds number from laminar to tempestuous. They take wound tapes of three distinctive wind proportions of 10.15, 7.95 and 3.4 for the investigation. They accept water as working liquid under the consistent warmth transition condition. Results demonstrates that the winding scored tube without curved tape yields most extreme warmth exchange upgrade of 400% in the laminar range and 140% in the tempestuous and the spirally furrowed tube with the turned tape indicates greatest warmth exchange improvement of 600% in the laminar range and 140% in the violent range. Warmth exchange execution of clockwise contorted tape with curve proportion of 7.95 is observed to be most extreme among all the three bend proportions.

T. Chinaruk et al. [10] have examined the impact of dimpled tube fitted with turned tape on the warmth exchange rate and the contact factor. The impacts of turn proportion and pitch on the weight misfortune and the normal warmth exchange coefficient for extensive variety of Reynolds number from 12,000 to 44,000. They played out the examination utilizing the two diverse dimpled tubes with various pitch proportions of dimpled surfaces and three turned tapes with various curve proportions (y/D) = 3, 5 and 7. They additionally analyze the warmth exchange rate and contact elements of both the basic tube and dimpled tube. The analyses result demonstrates that the dimpled tube with contorted tape embeds has the most extreme warmth exchange coefficient and rubbing factor as contrast with the straightforward tube with turned tape and dimpled tube without the bent tape. From the outcomes they found that with the

expansion of pitch proportion and abatement of the turn proportion, the warmth exchange coefficient and the erosion factor increment. The warmth exchange rate and grinding aspect in dimpled tube with curved tape with various turn proportions are 1.66, 3.03 and 6.31 times of those in the plain tube.

S.W. Hong and A.E. Bergles [11] have contemplated the impact of the contorted tape embed on the warmth exchange rate and the weight drop for the completely created laminar stream inside the tube. They take stream under the even tube with uniform pivotal warmth motion. The outcomes demonstrate that Nusselt number is an element of Reynolds number, PN and wind proportion of bent tape and the Nusselt numbers are gotten more prominent than 40. The outcomes demonstrate that the erosion factor is fundamentally rely on the Reynolds number. At the higher Reynolds number twirl stream builds the erosion factor because of which the weight drop additionally increments. The warmth exchangers can be decreased in measure by embeddings the curved tape inside the warmth exchanger.

P. Pongjet [12] have considered the impact of joined wire loop and turned tape embeds on the warmth exchange rate and the weight drop for the scope of the Reynolds number from 3000 to 18,000. The utilization of the joined wire curl with the curved tape impressively increment the weight drop and the warmth exchange rate be that as it may, the Nusselt numbers tends to diminish with ascent of the Reynolds number. On contrasting joined wire loop and curved tape turbulator with the smooth pipe at steady pumping power it is watched that the twofold increment in the warmth exchange execution is gotten particularly for the low Reynolds number. Along these lines, rather than utilizing smooth tube the tube with joined wire loop and wound tape ought to be utilized keeping in mind the end goal to acquire the better warmth exchange execution and this will prompt the most minimal warmth exchangers.

P. Murugesan *et al.* [13] have contemplated the impact of V-cut bent tape on the weight drop and the warmth exchange rate. They take turned tapes of three diverse bend proportions and three unique mixes of profundity and width proportions. The got consequences demonstrates V-cut wound tape offered higher rubbing factor, warm exchange rate and higher warm execution and the impact of profundity proportion is more overwhelming than that of width proportion for all the Reynolds number.

S.Al-Fahed et al. [14] have tentatively analyzed the impact of plain tube, tube with small scale

balance and tube with wound tape embeds on the weight drop and the warmth exchange coefficient. They take curved tape with three distinctive contort proportions apiece with two unique widths and information at Reynolds number well in laminar district. Oil is taken as working liquid inside the tube with uniform divider temperature. For the turn proportions of 5.4 and 3.6, the unyielding fit tape gives the superior qualities for warmth exchange than free fit. For turn proportion of 7.1, free fit geometry gives a higher estimation of warmth exchange than tight-fit one.

Chapter 3 : METHODOLOGY AND SIMULATION PROCEDURE

3.1 Computational Fluid Dynamics

Computational fluid dynamics utilizes the calculation and numerical techniques to fathom the principal equations of heat and mass exchange and fluid stream. In this thesis commercial CFD package ANSYS Fluent is used.

Fluent is utilizing for breaking down extensive variety of fluid flow tribulations together with laminar and turbulent flows, compressible and incompressible streams, viscous and in viscid streams, single stage and multi-stage streams and Newtonian and non-Newtonian streams. Likewise of these transient and enduring state analysis can be performed.

Fluent additionally utilizing for dissecting extensive variety of heat and mass exchange issues. By including just additional vitality condition conduction and convection issues can be effortlessly broke down. To recreate the more mind boggling wonders different models are accessible.

3.1.1 Governing Equations

Fluent investigates the fluid stream issues by fathoming the representing conditions with the assistance of numerical strategies. Conservation equation for mass and momentum are unraveled for all streams. By including the condition for the vitality preservation, the streams including heat exchange are broke down. Disturbance models are utilized to unravel extra transport conditions for tempestuous factors

3.1.1.1 Mass conservation

Mass conservation equation can be composed as takes after:

$$\frac{\partial \rho}{\partial t} + \nabla(\rho \vec{v}) = 0 \qquad (3.1.1)$$

3.1.1.2 Momentum conservation

The equation for momentum conservation is portrayed by:

$$\frac{\partial(\rho\vec{v})}{\partial t}+\nabla.(\rho\vec{v}\vec{v})=-\nabla p+\nabla.(\bar{\bar{\tau}})+\rho\bar{g}+\bar{F} \qquad (3.1.2)$$

where $\bar{\bar{\tau}}$ is the stress tensor, p is static pressure, $\rho\bar{g}$ is gravitational body force and F is the external forces including the user characterized source terms.

The stress tensor is defined as:

$$\bar{\bar{\tau}}=\mu\left[\left(\nabla\upsilon+\nabla\upsilon^{T}\right)-\frac{2}{3}\nabla\upsilon I\right] \qquad (3.1.3)$$

where **I** is the unit tensor and μ represents the molecular viscosity.

3.1.1.3 Energy conservation

The equation for the energy is describes by:

$$\frac{\partial}{\partial t}(\rho E)+\nabla.(\upsilon(\rho E+p))=\nabla.\left(k_{eff}\nabla T+(\bar{\bar{\tau}}_{eff}.\upsilon)\right) \qquad (3.1.4)$$

The right hand side terms stands for vitality exchange because of conduction and viscous dissipation, k_{eff} is effective thermal conductivity.

3.1.2 Finite Volume Method

Finite volume method is extremely valuable numerical technique utilized for descretizing the partial differential equations. It is utilized in the commercial CFD codes including Fluent. In finite volume method, space is separating into the number of control volumes and variable of intrigue is assessed at centroid of control volume. Volume indispensable is performed and utilizing uniqueness hypothesis changes over the disparity terms in the partial differential condition into a surface integral. At that point the surface necessary is assessed as transition at surface of each control volume. The motion going into a specific volume is equivalent to that leaving the nearby volume. Volume indispensable is performed and utilizing the uniqueness hypothesis changes over the disparity terms in the partial differential condition into a surface integral. It is utilized in the commercial CFD codes including Fluent.

3.1.3 QUICK

This method is weighted average of the second-order upwind and central difference, which can be give as:

$$\phi_{f}=\theta.\phi_{f,CD}+(1-\theta)\phi_{f,SOU} \qquad (3.1.5)$$

θ=1 results in a central difference scheme and θ = 0 yields a second-order upwind scheme. The usage in ANSYS Fluent utilizations variable and the arrangement subordinate estimation of θ. The The QUICK plan is more exact on the organized cross sections where remarkable upstream and downstream cells can be distinguished.

3.1.4 Turbulence Model

Turbulence can be specifically comprehended by the Navier-Stokes equations, yet computational cost of this approach is greatly high. Unravel the Reynolds Average Navier-Stokes (RANS) equation is substantially more pragmatic other option to demonstrate the choppiness. The essential thought of RANS is to break down speed into the time-found the middle value of term and change term:

$$u(x,y,z) = \bar{u}(x,y,z) + u'(x,y,z,t) \qquad (3.1.6)$$

The time normal of the change speed is zero and the mean speed is autonomous of time. RANS conditions can be effortlessly inferred by substituting decayed type of speed in the prompt Navier-Stokes condition:

$$\rho \bar{u}_j \frac{\partial \bar{u}_i}{\partial x_j} = \rho \bar{f}_i + \frac{\partial}{\partial x_j}\left[- p\delta_{ij} + \mu\left(\frac{\partial \bar{u}_i}{\partial x_j} + \frac{\partial \bar{u}_j}{\partial x_i} \right) - \rho \bar{u}_i \bar{u}_j \right] \qquad (3.1.7)$$

The right side of above equation represents to change of energy because of convection of mean stream. The change is equivalent to mean body constrain, thick pressure, isotropic pressure caused by mean weight field and pressure attributable to fluctuating speed field (Reynolds stretch). To accomplish the conclusion of RANS condition it requests extra displaying. Different systems have been proposed, extending from straightforward one-condition models, for example, Spalart-Allmaras, to confounded Large Eddy Simulation.

ANSYS Fluent gives two condition models which are normally utilized for the handy designing applications among the assortment of other disturbance models. To speak to the impact of the disturbance on the mean stream, two extra transport conditions are incorporated into two-condition models. The primary condition comprehends for disturbance motor vitality k that decides choppiness force and the second condition shifts between the diverse models. In the

k-ε show, it is the choppiness motor vitality dissemination rate and in the k-ω display, it is particular dispersal rate (ω).

In present study, Reynolds number is well inside tempestuous administration subsequently the k-ε demonstrate is utilized in light of the fact that the k-display is by and large a high Reynolds number model and shear-push transport (SST) k-ω show is for the most part utilized for low Reynolds number stream issues. Feasible k-demonstrate is an alteration in view of the standard k-display, in this manner more exact and solid. The conditions for the disturbance dynamic vitality and active vitality dissemination rate are:

$$\frac{\partial(\rho k)}{\partial t}+\frac{\partial(\rho k v_j)}{\partial x_j}=\frac{\partial}{\partial x_j}\left[\frac{\mu_T}{\sigma_k}\frac{\partial k}{\partial x_j}\right]+2\mu_T S_{ij}S_{ij}-\rho\varepsilon \qquad (3.1.8)$$

$$\frac{\partial(\rho\varepsilon)}{\partial t}+\frac{\partial(\rho\varepsilon v_j)}{\partial x_j}=\frac{\partial}{\partial x_j}\left[\frac{\mu_T}{\sigma_\varepsilon}\frac{\partial \varepsilon}{\partial x_j}\right]+C_{1\varepsilon}\frac{\varepsilon}{k}2\mu_T S_{ij}S_{ij}-2C_{2\varepsilon\rho}\frac{\varepsilon^2}{k} \qquad (3.1.9)$$

3.1.5 Validation

In order to approve the commercial algorithm, Computational fluid dynamics (CFD) reenactments are completed for the laminar and fierce incompressible liquid stream in benchmark issues, for example, lid driven cavity (100< Re< 5000) and in reverse confronting step (0.0001< Re<100).

3.1.5.1 Lid Driven Cavity

In this problem, the proportion of stature to width of cavity is taken as 1.0, as appeared in Figure 3.1. A commercial CFD package, ANSYS FLUENT was utilized to examine and envision the stream inside the cavity of viewpoint proportion 1. The recreation results are introduced as far as speed profiles and stream shapes. Speed profile for square cavity was observed to be in great concurrence with past exploratory outcomes. Such numerical strategy for the two dimensional unfaltering incompressible Navier-Stokes conditions are frequently utilized for the code approval. No-slip speed limit condition (u = v = 0) is connected on every one of dividers, with exception of the best top. On best top (U= 1 and V = 0) is connected. The base limit of space is displayed as divider.

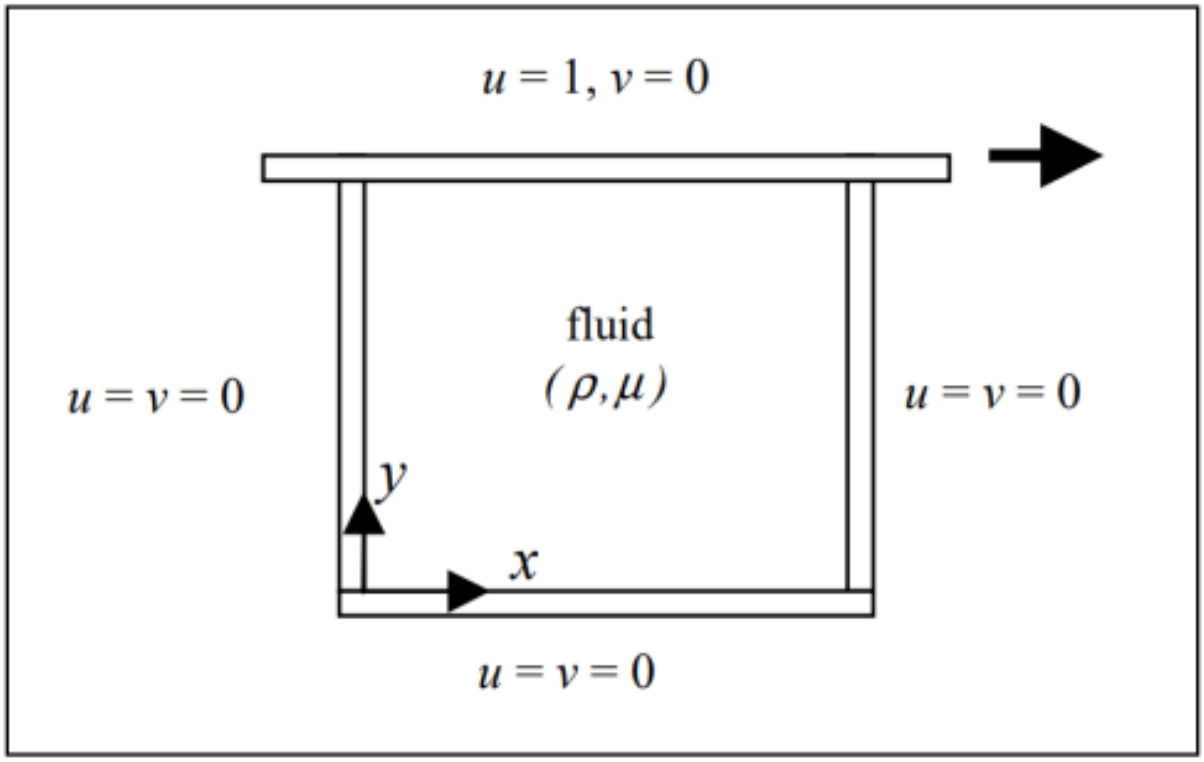

Figure 3.1: Classical problem of lid driven cavity flow (Ghia et al.[23])

Figure 3.2 demonstrates the V-speed profile along the even line going through geometric focus of square pit for angle proportion (AR=1) for the laminar district (Re = 100 and 400). As can be seen there is an amazing understanding in speed profile between CFD reenactments in this investigation and trial estimated by Ghia et al. [23] It was discovered that flow and structure of essential vortex are unequivocally influenced by RN for a similar viewpoint proportion of the depression. It was discovered that structure and progression of the essential vortex are firmly influenced by the Reynolds number for a similar viewpoint proportion of the hole.

Correlation of the ANSYS FLUENT recreation results with test information approve the industrially accessible programming ANSYS FLUENT in giving a sensible decent arrangement of entangled stream structures, incorporating stream with partition. No-slip speed limit condition (u = v = 0) is connected on every one of the dividers, aside from the best top. On the best top (U= 1 and V = 0) is connected. The base limit of space is displayed as divider.

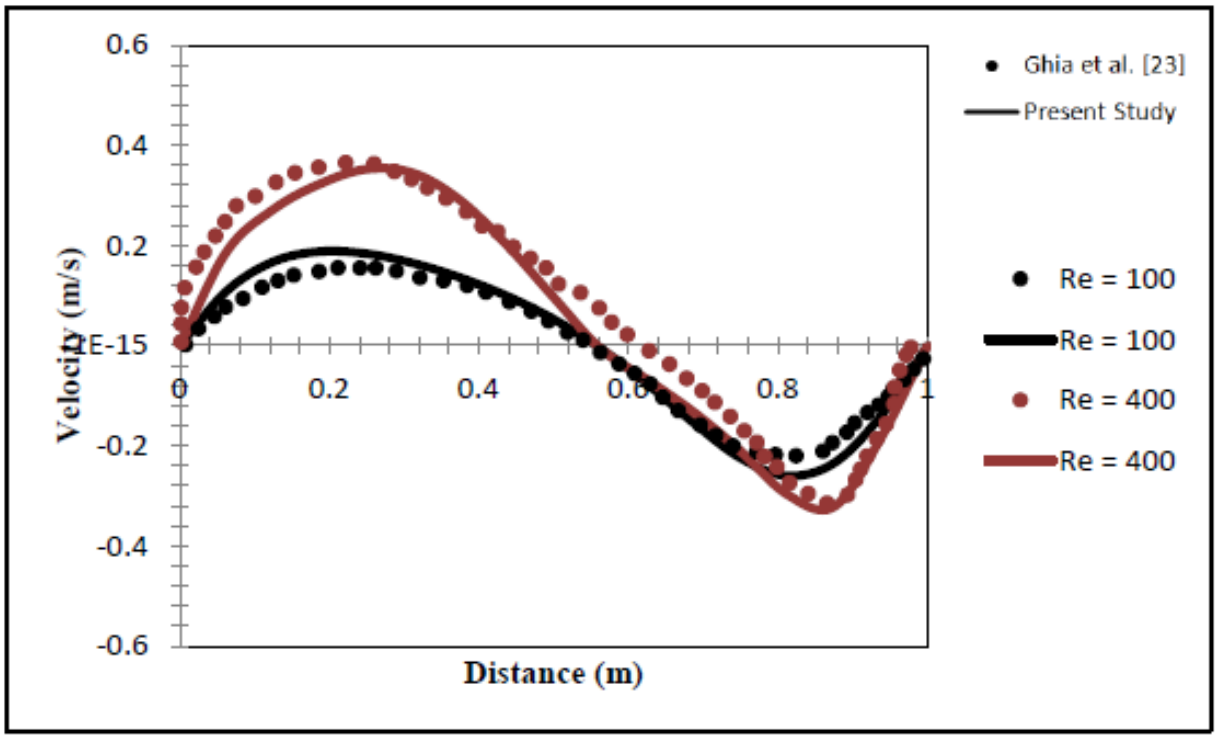

Figure 3.2: V- velocity profile at horizontal line passing through geometric centre at different Reynolds number (Laminar Region)

To visualize the general stream designs, from the computational information the speed profile plots for viewpoint proportion (AR=1) at Reynolds number (Re = 3200) is appeared in Figure 3.3. It demonstrates the V-speed profile along the even line going through geometric focal point of square hole for angle proportion (AR=1) for the violent locale (Re = 3200). As can be seen there is a magnificent assention in speed profile between CFD reproductions in this examination and trial estimated by Ghia et al. It was discovered that structure and progression of the essential vortex are emphatically influenced by Reynolds number for a similar viewpoint proportion of the depression. Correlation of the ANSYS FLUENT reenactment results with trial information approve the economically accessible programming ANSYS FLUENT in giving a sensible decent arrangement of muddled stream structures, incorporating stream with partition.

No-slip velocity boundary condition (u = v = 0) is connected on dividers, aside from best cover. On best top (U= 1 and V = 0) is connected and base limit of space is displayed as divider. The perceptible factors of enthusiasm for ordinary numerical strategies, for example, speed and weight are typically acquired by understanding the Navier-Stokes condition. Such numerical strategy for the two dimensional enduring incompressible Navier-Stokes conditions are frequently utilized for the code approval.

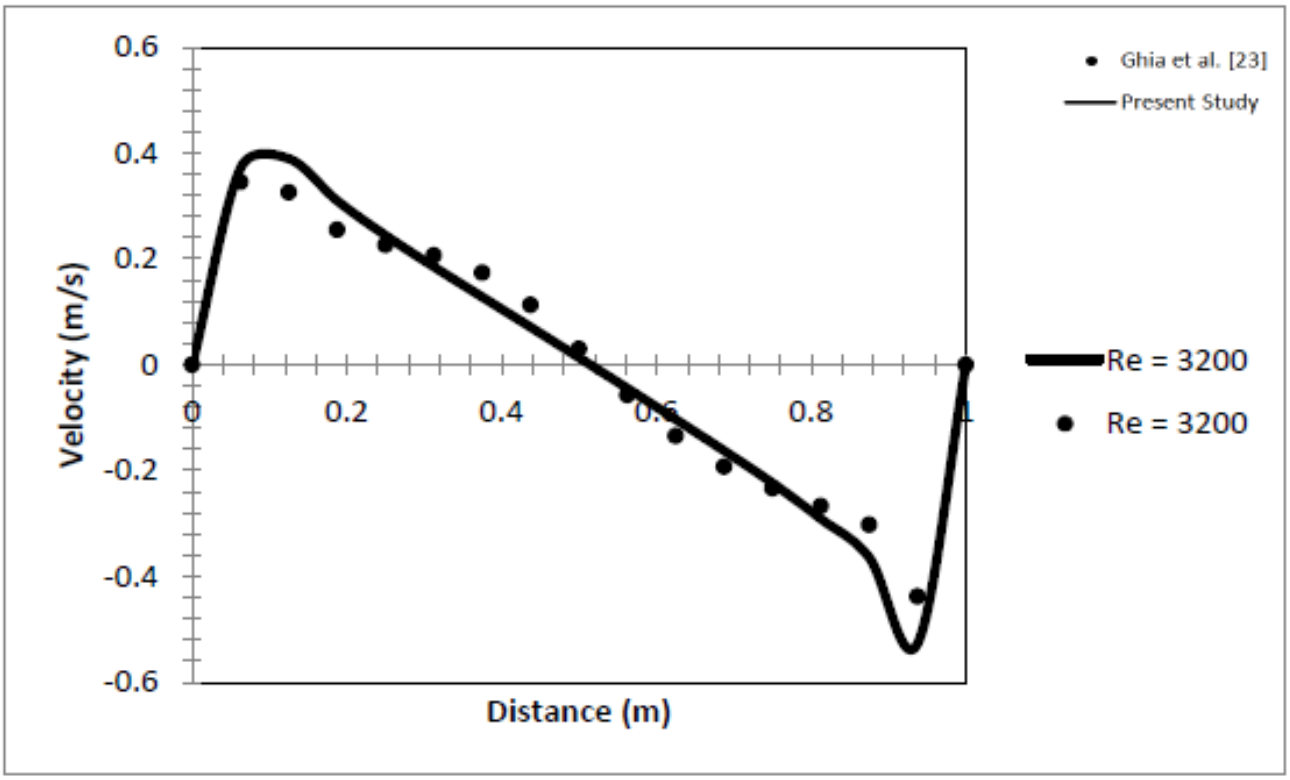

Figure 3.3: V- velocity profile at horizontal line passing through geometric centre at different Reynolds number (Turbulent Region)

Figure 3.4 demonstrates the U-speed profile along the vertical line going through geometric focal point of square cavity for viewpoint proportion (AR=1) for the laminar locale (Re = 100 and 400). As can be seen there is a magnificent understanding in speed profile between CFD reenactments in this investigation and trial estimated by Ghia et al. It was discovered that structure and elements of the essential vortex are emphatically influenced by Reynolds number for a similar perspective proportion of the hole. No-slip speed limit condition (u = v = 0) is connected on dividers, aside from best top. On the best cover (U= 1 and V = 1) is connected and base limit of space is demonstrated as divider.

The macroscopic variables of enthusiasm for ordinary numerical techniques, for example, speed and weight are generally acquired by understanding the Navier-Stokes condition. Such numerical technique for the two dimensional relentless incompressible Navier-Stokes conditions are frequently utilized for the code approval. Examination of ANSYS FLUENT reenactment results with trial information approve the industrially accessible programming ANSYS FLUENT in giving a sensible decent arrangement of convoluted stream structures, incorporating stream with partition.

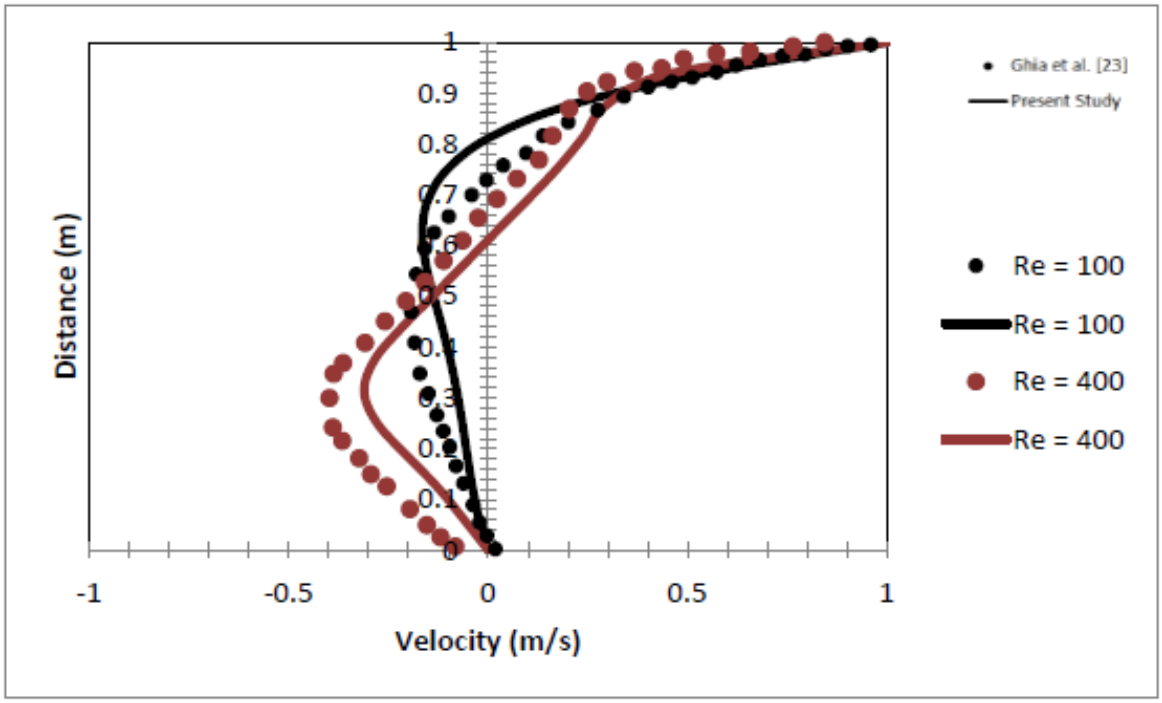

Figure 3.4: Velocity profile at vertical line passing through geometric centre at different Reynolds number (Laminar Region)

To envision the general stream designs, the speed profile plots from the computational information for perspective proportion (AR=1) at Reynolds number (Re = 3200) is appeared in Figure 3.5. It demonstrates the U-speed profile along the vertical line going through geometric focus of square cavity for perspective proportion (AR=1) for the violent locale (Re = 3200). The naturally visible factors of enthusiasm for customary numerical strategies, for example, speed and weight are generally acquired by settling the Navier-Stokes condition. Such numerical strategy for the two dimensional enduring incompressible Navier-Stokes conditions are frequently utilized for the code approval. Correlation recreation results with the approved exploratory information approve the industrially accessible programming ANSYS FLUENT in giving a sensible decent arrangement of confused stream structures, incorporating stream with detachment. No-slip speed limit condition (u = v = 0) is connected on dividers, aside from best top. On the best top (U= 1 and V = 0) is connected and base limit of area is demonstrated as divider.

As can be seen there is a great understanding in speed profile between CFD reenactments in this investigation and trial estimated by Ghia et al.[23] It was discovered that progression and structure of essential vortex are emphatically influenced by Reynolds number for a similar viewpoint proportion of the hole.

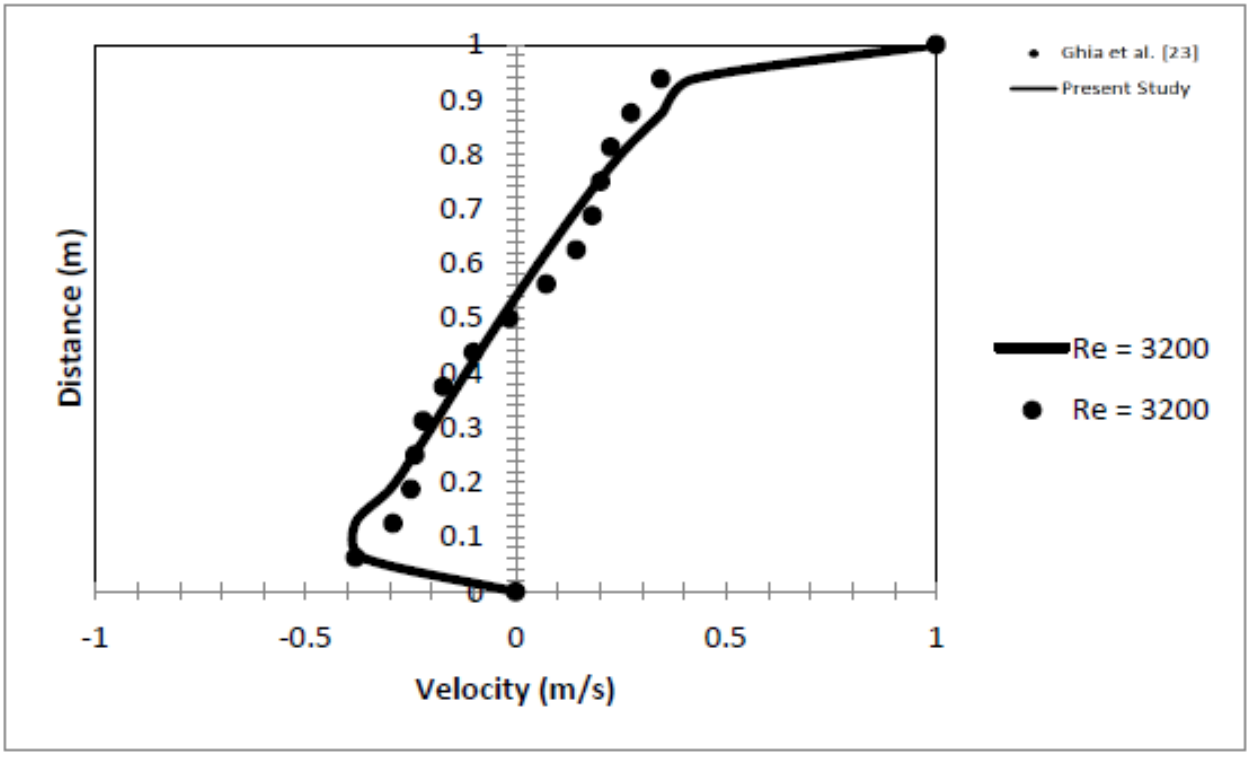

Figure 3.5: Velocity profile at vertical line passing through geometric centre at different Reynolds number (Turbulent Region)

3.1.5.2 Backward Facing Step

In order to validate the commercial algorithm, Computational fluid dynamics (CFD) simulations are carried out for the laminar and turbulent incompressible fluid flow in benchmark problems i.e. backward facing step ($0.0001 < Re < 100$).

Sketch of the flow configuration and definition of length scales (G. Biswas et al.[24]) is shown in Figure 3.6, h is height of channel upstream of step which is taken as 1 m, S is the step height which is taken as 2 m, L is the channel length of the upstream of the step and L_d is the channel length of downstream of the step which are taken as 3 m and 4 m respectively. In order to simulate a fully developed laminar channel flow upstream of the step, a standard parabolic velocity profile with a velocity of 1 m/s is prescribed at the channel inlet for the two-dimensional model. S is the step height which is taken as 2 m, L is the channel length of the upstream of the step and L_d is the channel length of downstream of the step which are taken as 3 m and 4 m respectively. S is the step height which is taken as 2 m, L is the channel length of the upstream of the step and L_d is the channel length of downstream of the step.

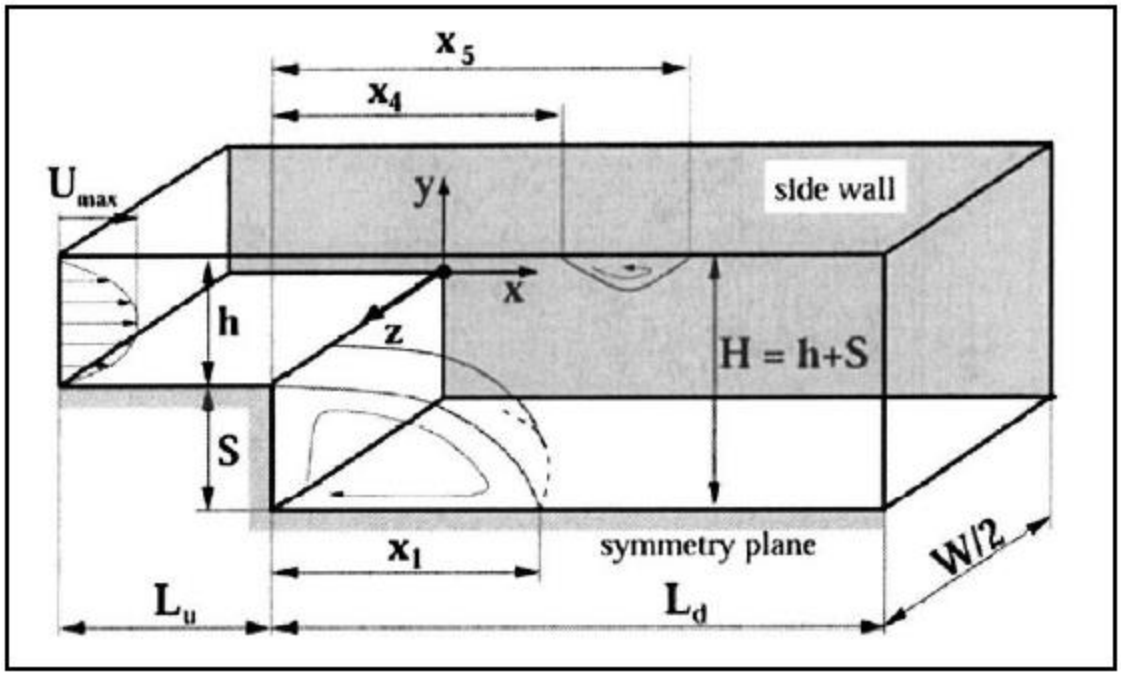

Figure 3.6: Sketch of the flow configuration and definition of length scale (G.Biswas et al.[24])

The measure of the primary whirlpool is almost steady for all the Reynolds number underneath (Re = 1) as appeared in the Figure 3.7. The length x_1 of main corner vortex behind re-flow area is standardized by the progression stature S as a component of Reynolds number (Re). The vortex unequivocally increments in measure for the Reynolds number (Re > 1). The span of the distribution area consistently increments with expanding the Reynolds number. As can be seen there is a brilliant understanding in the Length x_1 of main corner whirlpool behind regressive confronting step standardized by progression tallness S plot between ANSYS FLUENT recreations in this and examination and the exploratory estimated by G. Biswas et al. [24]

It was discovered that elements and structure of essential vortex are unequivocally influenced by RN. Examination reproduction results with exploratory information approve the industrially accessible programming ANSYS FLUENT in giving a sensible decent arrangement of confused stream structures, incorporating stream with partition. On the channel stream upstream of progression, a standard allegorical speed profile (U= 1 and V = 0) is connected at the channel delta for the two-dimensional model. The base limit of the space is displayed as divider. Examination reproduction results with exploratory information approve the industrially accessible programming ANSYS FLUENT in giving a sensible decent arrangement of confused stream structures, incorporating stream with partition.

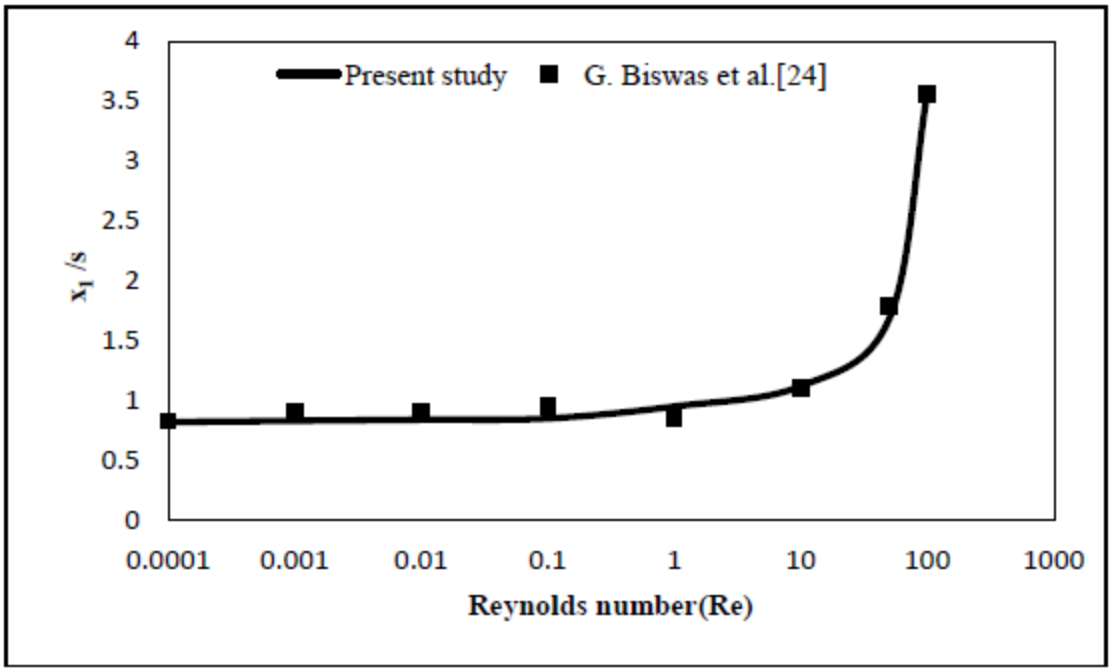

Figure 3.7: Length x_1 of the first corner eddy behind the backward facing step normalized by the step height S.

3.1.6 Numerical Details

Table 3.1 lists the detailed numeric used in simulation.Actual design of the pipe joint assembly has been taken for simulation using Computational Fluid Dynamics. Results obtained from CFD simulation are compared with experimental results. Further some other design changes (such as changing diameter of tube, length of tube, insert the twisted tape of different twist ratios and different clearance ratio inside the tube) have been simulated for same mass flow rate and compared with actual design.

Table 3.1: Detailed numerical methods used in simulation

Code	**ANSYS FLUENT**
Turbulence model	Realizable k- ε
Velocity-Pressure Coupling	SIMPLE
Gradient	Least Squares Cell Based
Momentum	QUICK
Pressure	Body Force Weighted
Turbulent Kinetic Energy	QUICK
Specific Dissipation Rate	QUICK
Energy	QUICK

Simulation has been performed on pipe joint assembly by using commercial CFD (Computational Fluid Dynamics) code Fluent was performed under following methodology:

- Simulation has been performed on pipe joint assembly and results are validated with the theoretical results for the actual geometry.
- Grid independent test has been performed and optimum grid size has been found for the geometry.
- Simulation has been done using different model by changing the diameter and length of the same pipe joint assembly and compares the performance parameters for all three cases.
- Simulation is performed by insert the twisted tape of different twirl ratios and consent ratios inside the tube and compares performance parameters for all the cases.
- After doing the above steps, best design of PJA has been obtained that could maximize the rate of heat transfer at lower cost and improve the energy efficiency of refrigerator.

3.2 Simulation Procedure

Actual design of the pipe joint assembly has been taken for simulation using Computational Fluid Dynamics. Results obtained from CFD simulation are compared with experimental results. Further some other design changes (such as changing diameter of tube, length of tube, insert the twisted tape of different twist ratios and different clearance ratio inside the tube) have been simulated for same mass flow rate and compared with actual design. The major geometrical dimensions and simulation procedure is explained below.

3.2.1 Geometrical Details of Actual Design of PJA

In domestic refrigerator, De-Super-heater which is also called as Pipe Joint Assembly (PJA), is a serpentine tube which is immersed in tray-drip and connecting compressor outlet and condenser inlet. It is used to desuperheat the super heated refrigerant vapor coming out from the compressor and also used to evaporate the defrost water in the tray drip. In domestic refrigerator, De-Super-heater which is also called as Pipe Joint Assembly (PJA), is a serpentine tube which is immersed in tray-drip and connecting compressor outlet and condenser inlet. It is used to desuperheat the super heated refrigerant vapor coming out from the compressor and also used to evaporate the defrost water in the tray drip.

Geometry of the pipe joint assembly (PJA) was modeled in UNIGRAPHICS NX, licensed in LG Soft PVT LTD. using geometric details given in Table 3.2. Geometry consists of a tray drip inside which the pipe joint assembly (PJA) is placed tube which is made of copper and insulation is provided above this tube using PVC shrink. In the tray drip the stagnant water of initial temperature of $XX^{o}C$ is present and the tube has one inlet and one outlet. In this case one row of the pipe joint assembly is outside the water.

Modelling Assumptions:

To simulate the PJA some assumptions were assumed and given below:

- Continuum Approximation
- Steady State Condition
- Viscosity is independent of shear rate.
- Boundary conditions are no slip condition.
- Tube has uniform diameter throughout the length
- Tube has smooth surfaces
- Specific heat (C_p) of refrigerant remains constant
- Temperature of the stagnant water remains constant
- All the properties of refrigerant and water are independent of temperature.

Properties of iso-butane, copper, PVC and water:

The superheated iso-butane vapor coming from the compressor is passed through the PJA before going to condenser and is cooled by the defrost water. The PJA is made of copper and PVC. Properties of copper, PVC and iso-butane used in the simulation are given in the Table 3.2.

Table 3.2: Properties of Iso-butane, copper, PVC and water

Property	Unit	Iso butane	Copper	PVC	Water
Density	Kg/m^3	17.6	8978	1300	998.2
Specific heat	J/kg-K	2017	381	1000	4182
Thermal Conductivity	W/m-K	0.01978	401	0.19	0.6
Dynamic Viscosity	Kg/m-s	8.22×10^{-6}	N.A.	N.A.	0.001003

Boundary Conditions:

Mass flow rate and temperature of superheated refrigerant vapor were specified at the inlet. The

thickness of the tube is neglecting during the geometrical modelling. To account this, shell conduction boundary condition had been taken for both copper and PVC shrink. The value of operating parameters was specified in Table 3.3.

Table 3.3: Boundary conditions

Fluid	Inlet mass flow rate(gm/s)	Outlet Pressure, Pa (gauge)	Inlet Temperature (^oC)	Turbulent intensity (%)	Hydraulic diameter (m)
Iso-butane	0.84	0	50	5	0.00336

3.3 Description of different designs

In addition to the simulation of actual design, additional designs were obtained by changing the geometrical parameters such as diameter, length of the tube and insert the twisted tape inside the tube. All the designs were simulated using CFD and their detailed description is given below.

3.3.1 Change in diameter and length of tube

A quantity of interest in the analysis of tube flow is the pressure drop since it is directly related to the compressor power requirement to maintain the flow. To increase the energy efficiency of the system we have to reduce the compressor power requirement by reducing the pressure drop without compromising to the total heat transfer rate. So we increase the diameter of pipe by keeping the same surface area of the tubes. Also, when we increase the diameter by keeping the total surface area constant the length of the pipe joint assembly get reduced because of which more surface area of pipe joint assembly would dip in the water. We took two model PJA-1 and PJA-2 with XX mm diameter and XX mm diameter respectively and had done the CFD simulation to see the effect of changing diameter on pressure drop and heat transfer rate.

3.3.1.1 Geometrical Details of modified design of PJA (PJA-1)

To increase the energy efficiency of the system we have to reduce the compressor power requirement by reducing the pressure drop without compromising to the total heat transfer rate. Diameter of the PJA has been increased from XX mm to XX mm and the length of the PJA is decreased from XX mm to XX mm for keeping the same surface area and named it as PJA-1. Geometry of PJA-1 was modelled in UNIGRAPHICS NX, licensed in LG Soft PVT. LTD. Geometry consists of a tube which is made of copper and the insulation is provided above this

tube using PVC shrink.

PJA-1 is a serpentine tube which is immersed in tray-drip and connecting compressor outlet and condenser inlet. It is used to desuperheat the super heated refrigerant vapor coming out from the compressor and also used to evaporate the defrost water in the tray drip. In this case, all the pipe joint assembly-1 (PJA-1) is dip in water as compared to the actual case so in this case we get more contact surface between the tube and water so more will be the heat transfer take place in this case as compare to the actual design. In the tray drip the stagnant water of initial temperature of XX^{o}C is present and the tube has one inlet and one outlet. We use same assumptions, working fluid and the boundary conditions in this case also which we use in actual case.

3.3.1.2 Geometrical Details of modified design of PJA (PJA-2)

Diameter of the PJA has been increased from XX mm to XX mm and the length of the PJA is decreased from XX mm to XX mm for keeping the same surface area and named it as PJA-2. Diameter increased to increase energy efficiency of system and reduce compressor power requirement by reducing the pressure drop without compromising to the total heat transfer rate.

Geometry of PJA-2 was modelled in UNIGRAPHICS NX, licensed in LG Soft PVT. LTD. Geometry consists of a tube which is made of copper and insulation is provided above this tube using PVC shrink. The pipe joint assembly is placed in the tray drip and all the pipe joint assembly-2 (PJA-2) is dip in the water. In this case we get maximum contact surface between the tubes and water so maximum will be the heat transfer take place with minimum pressure drop in this case as compare to the previous design. In the tray drip the stagnant water of initial temperature of XX^{o}C is present and the tube has one inlet and one outlet. We use same assumptions, working fluid and the boundary conditions in this case also which we use in actual case. The pipe joint assembly is placed in the tray drip and all the pipe joint assembly-2 (PJA-2) is dip in the water. In this case we get maximum contact surface between the tubes and water.

3.3.2 Tube with Twisted Tape Turbulators

Twisted tape turbulators are formed with the metal tape by twisting with mechanical means and these twisted tape type turbulators spawn swirling flow and cause enhanced flowing assimilation involving nearly wall zone and central section at expense of an increased pressure drop so, the warmth relocate in tubes can be improved by fluid assimilation without the need of any external

power source. The most well known twisted tape design is full length twisted tape. We insert six different twisted tapes with three different clearances ratios (c/D = 0.166, 0.272 and 0.4) and different twist ratios (y/D = 5, 6 and 7) inside tube in order to see the effect of these parameters on warmth relocate speed and the pressure drop. The Geometry of the different twisted tapes with different twist ratios and different clearance ratios are shown in Figure 3.6 and Figure 3.7 respectively.

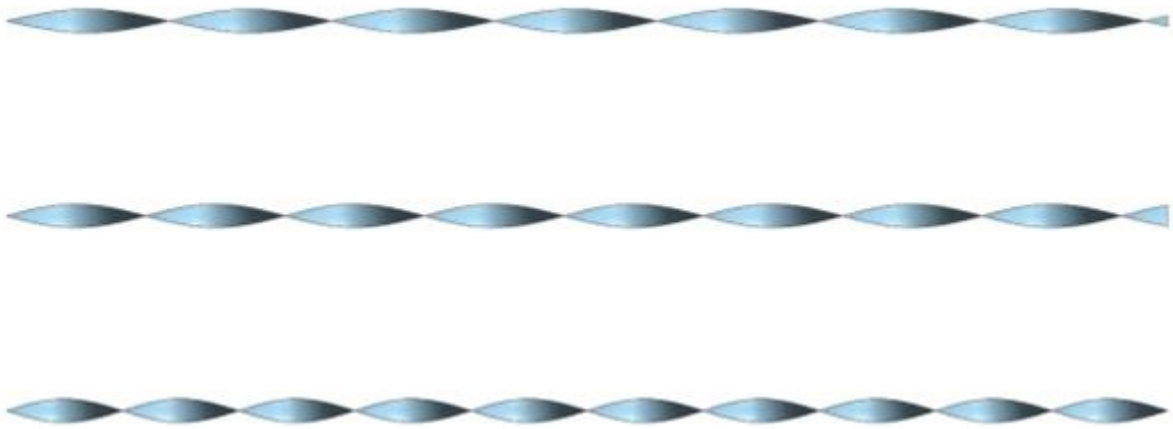

Figure 3.8: Geometry of different full length twisted tape (3-D view)

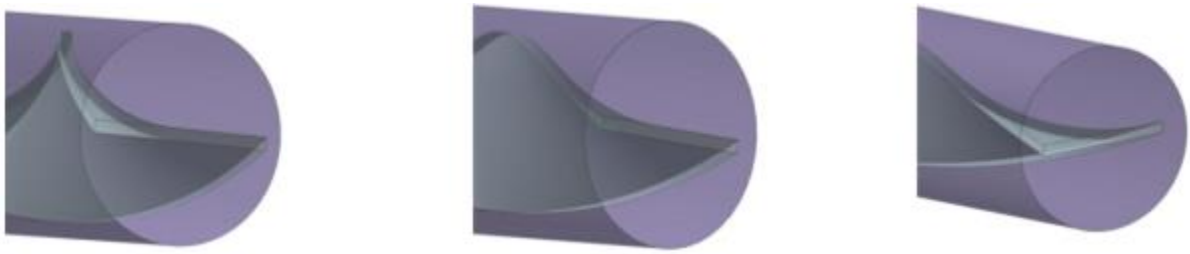

Figure 3.9: Geometry of different FLTT with different clearance ratios (3-D view)

3.3.2.1 Geometric details of PJA-2 with twisted tape turbulators

Turbulence causes enhanced fluid assimilation amid nearly wall section and central section at expense of an increased pressure drop so, the warmth relocate in tubes can be improved by fluid assimilation without the need of any external power source. Twisted tape turbulators insert inside the PJA-2 to enhance the warmth relocate speed inside the tube and named it as PJA-2 with twisted tape turbulators. We insert six different twisted tapes with three different clearances ratios (c/D = 0.166, 0.272 and 0.4) and different twist ratios (y/D = 5, 6 and 7) inside the tube in order to see the effect of these parameters on warmth relocate speed and the pressure drop at the

different mass flow rates. Geometry of PJA-2 with twisted tape turbulators was modelled in UNIGRAPHICS NX, licensed in LG Soft PVT. LTD.

Geometry consists of a tube which is made of copper and insulation is provided above this tube using PVC shrink. The pipe joint assembly with the twisted tapes of dissimilar twirl ratios and clearance ratios is placed in tray drip and all pipe joint assembly dip in water so in this case we get maximum contact surface between the tubes and water so maximum will be the heat transfer take place in this case as compare to the actual design. In the tray drip the stagnant water of initial temperature of $XX^{o}C$ is present and the tube has one inlet and one outlet. We use same assumptions, working fluid and the boundary conditions in this case also which we use in actual case.

Twisted tape of different twist ratios (y/D = 5, 6 and 7) are chosen for the study in order to see the variation in warmth relocate speed and pressure drop inside tube at the different mass flow rates ($\dot{m}$ = XX gm/s, XX gm/s and XX gm/s). Out of these three twist ratios only one twist ratio will be finalized for the final design. According to the commercial CFD software ANSYS FLUENT which twisted tape of particular twist ratio gives optimize results that will be finalized for the final design. Also the effect of the three dissimilar clearance ratios (c/D = 0.166, 0.272 and 0.4) on the warmth relocate speed and the pressure drop inside the tube at the different mass flow rates will be studied and according to the commercial CFD software ANSYS FLUENT which twisted tape of particular clearance ratio gives optimizes results will be chosen for the final design. Out of these three twist ratios only one twist ratio will be finalized for the final design. According to the commercial CFD software ANSYS FLUENT which twisted tape of particular twist ratio gives optimize results that will be finalized for the final design. Twisted tape of different twist ratios) are chosen for the study in order to see the variation in warmth relocate speed and pressure drop inside tube at the different mass flow rates.

Chapter 4 :CFD SIMULATION RESULTS AND COMPARISON OF DIFFERENT DESIGNS

In domestic refrigerator, De-Super-heater which is also called as Pipe Joint Assembly (PJA), is a serpentine tube which is immersed in tray-drip and connecting compressor outlet and condenser inlet. It is used to desuperheat the super heated refrigerant vapor coming out from the compressor and also used to evaporate the defrost water in the tray drip. The use of De-super-heater or pipe joint assembly (PJA) for the cooling of superheated refrigerant vapor has been increased in past few decades. In spite of its application in almost all industrial applications, not that much of work has been reported to date on such type of heat exchangers. So, efforts have been made here, to simulate such systems using commercial CFD (Computational Fluid Dynamics) algorithm, ANSYS FLUENT and results of simulations are presented. Also, a parametric study was performed to estimate the effect of PJA tube diameter and PJA length by keeping the surface area constant and insert the twisted tape of different twist ratios and clearance ratios inside tube for different mass flow rates.

4.1 Effect of Tube Diameter

Diameter of the PJA has been increased and the length of the PJA is decreased for keeping the same surface area and its effects have been studied on the outlet temperature, warmth relocate speed and the pressure drop for different mass flow rates. We take three different Pipe Joint Assembly (PJA) tubes and named it as PJA, PJA-1 and PJA-2 with the outer diameters (D 2) = XX mm, XX mm and XX mm respectively. The thickness of PJA is taken as XX mm and thickness of PJA-1 and PJA-2 is taken same as XX mm. The effect of diameter on the warmth relocate speed and the pressure drop have been deliberate with help of commercial CFD (Computational Fluid Dynamics) algorithm, ANSYS FLUENT and the CFD results are validated with the theoretical results for the heat transfer rate which shows very good agreement with each other. The curve between the mass flow rate and the heat transfer rate are shown in Figure 4.1 for the different diameters. It can be seen from the Figure 4.1, as the diameter increase and the length decrease to keep the same surface area, the heat transfer rate remain same for all the mass flow rates ($\dot{m}$ = XX gm/s, XX gm/s and XX gm/s). From the Figure 4.1, we can also observe that as we increase mass flow rate at tube inlet, heat transfer rate also increase which shows very good agreement with the theoretical results.

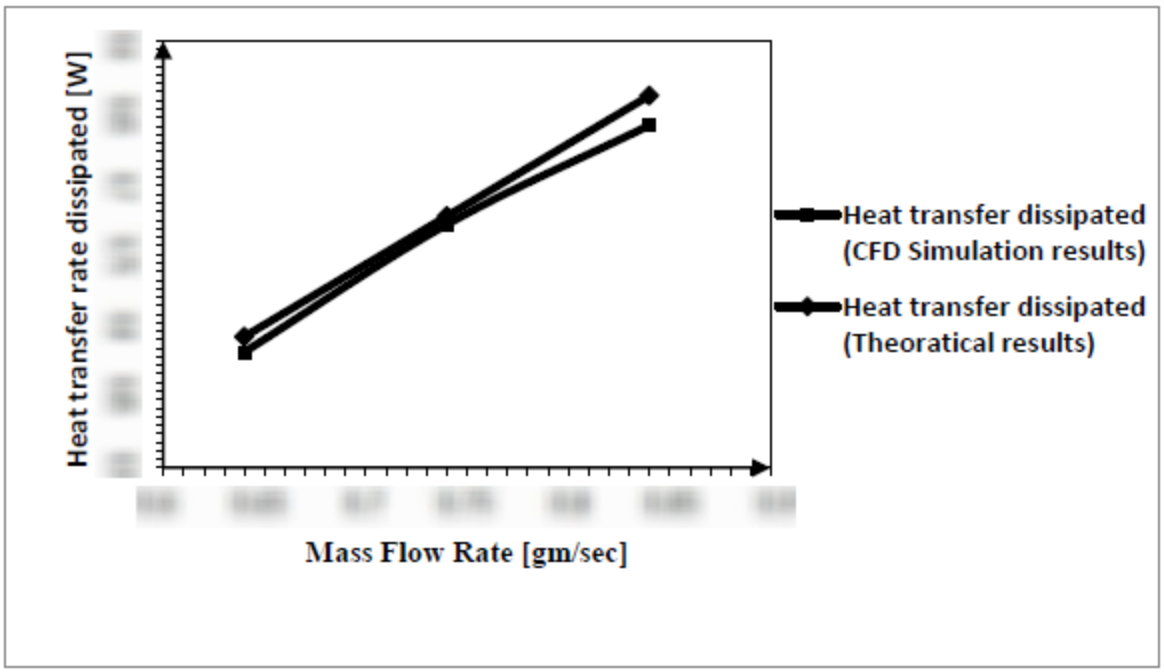

Figure 4.1: Heat transfer rate dissipated versus mass flow rate

Figure 4.2 shows the pressure drop for the plain tube with three different diameters. It can be seen from Figure 4.2, as diameter increase and length decrease to keep the same surface area, the pressure drop reduces significantly for all the mass flow rates. From the results we found that as we increase the inlet mass flow rate, the warmth relocate speed and the pressure drop values are also increases.

For same surface area of tubes with different diameters, the total heat transfer rate is same for all the mass flow rates (ṁ = XX gm/s, XX gm/s and XX gm/s). From the results we found that with the increase of the diameter, the pressure drop reduces significantly for all the mass flow rates (ṁ = XX gm/s, XX gm/s and XX gm/s). The pressure drop in the tube with different outer diameter (D = XX mm and XX mm) are 0.07 and 0.016 times respectively of those in the actual tube of XX mm diameter. The thermal performance improvement for the different diameters (D = XX mm and XX mm) are 2.42 and 3.94 respectively. So the tube with the XX mm diameter gives us the maximum thermal performance improvement as compared to the other cases. From the results we found that with the increase of the diameter, the pressure drop reduces significantly for all the mass flow rates.

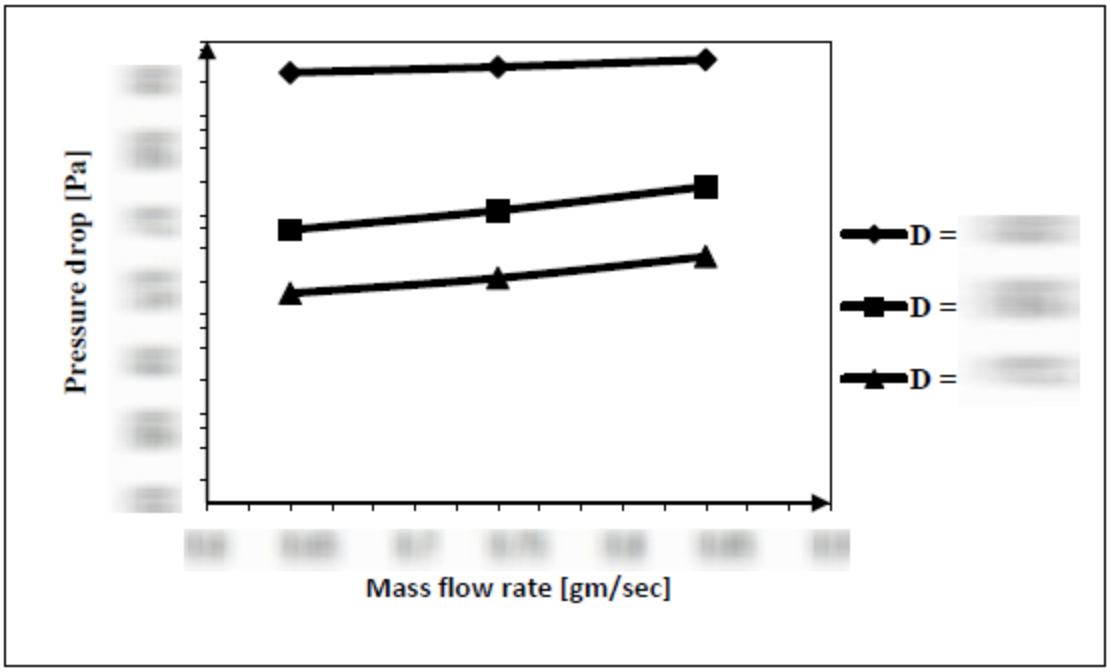

Figure 4.2: Pressure drop versus mass flow rate for different diameters

4.2 Effect of Twist Ratio of Twisted Tape

Twist ratio of the twisted tape turbulators has been varied inside the tube and its effects has been studied on outlet temperature, warmth relocate speed and the pressure drop for different mass flow rates. We take the three different values of the twist ratios (y/D) = 5, 6 and 7 in order to study its effects with the help of commercial CFD (Computational Fluid Dynamics) algorithm, ANSYS FLUENT. The curve between mass flow rate and pressure drop are shown in Figure 4.3 for the different twist ratios. It can be seen from the graph, as the twist ratio has increase, the pressure drop is decreased for all the mass flow rates (ṁ = XX gm/s, XX gm/s and XX gm/s) and this variation shows the good agreement with the literature review.

Turbulence causes enhanced fluid assimilation between nearly wall section and central section at expense of an increased pressure drop so, the warmth relocate speed in tubes can be improved by fluid assimilation without the need of any external power source. It can be seen from the graph, as the twist ratio has increase, the pressure drop is decreased for all the mass flow rates (ṁ = XX gm/s, XX gm/s and XX gm/s) and this is due to fact that with increase in the twist ratios (y/D = 5, 6 and 7) of the twisted tape, the swirl motion in the flow goes down which leads to decrease in the pressure drop. It can be seen from the graph, as the twist ratio has

increase, the pressure drop is decreased for all the mass flow rates and this variation shows the good agreement with the literature review.

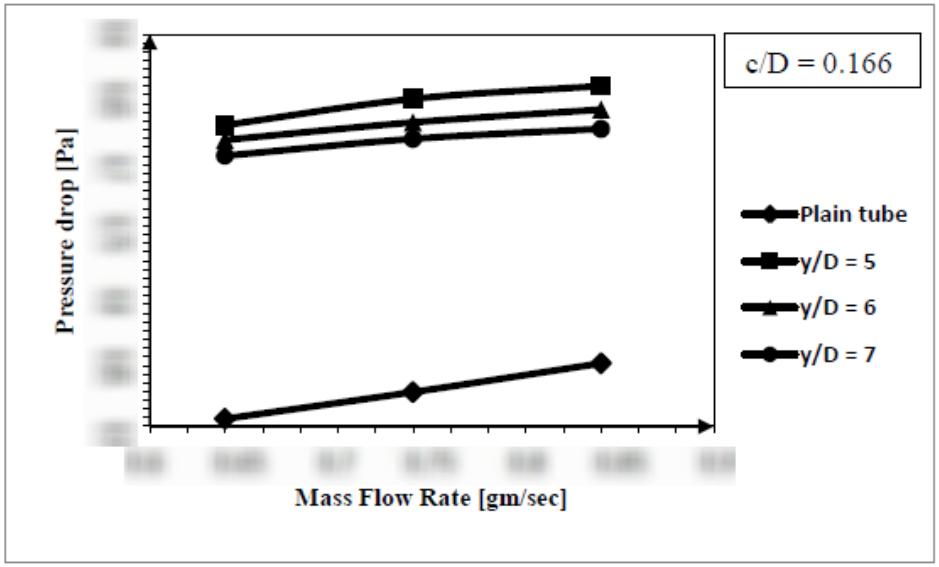

Figure 4.3: Pressure drop versus mass flow rate for different twist ratios

Figure 4.4 shows the variation heat transfer rate for the tube with and without the twisted tapes of dissimilar twist ratios.

From consequences we found that as we increase inlet mass flow rate, the warmth relocate speed and the pressure drop values also increases. We found that with diminish of twist ratio, the heat transfer rate and the pressure drop increase.

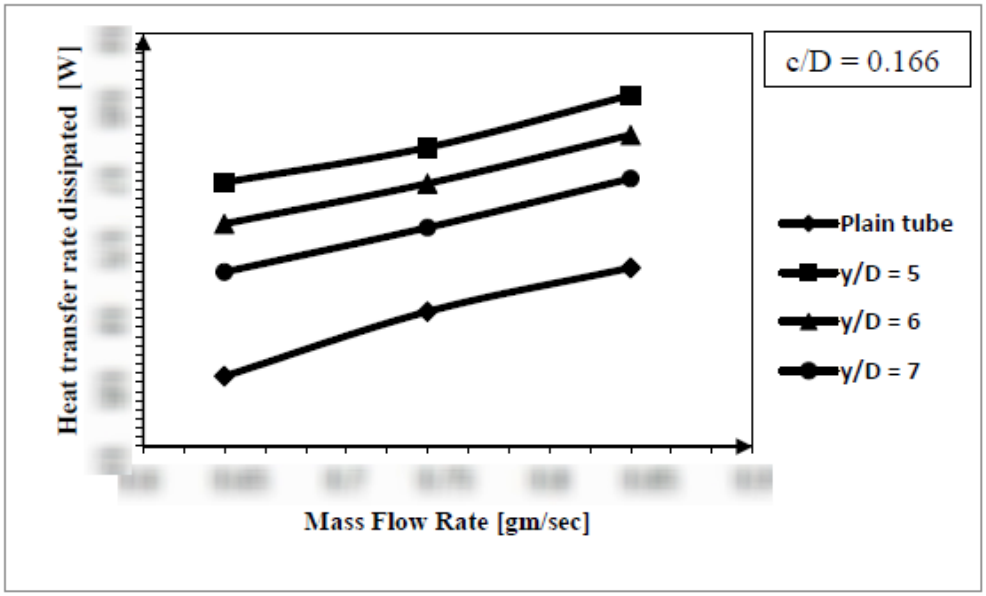

Figure 4.4: Heat transfer rate dissipated versus mass flow rate for different twist ratios

The heat transfer rate in tube with twisted tape with different twist ratios (y/D = 5, 6 and 7) are 1.33, 1.25 and 1.17 times respectively of those in plain tube. The pressure drop value in tube with twisted tape of different twist ratios (y/D = 5, 6 and 7) are 2.84, 2.68 and 2.56 times respectively of those in the plain tube and the thermal performance improvement for the different twist ratios (y/D = 5, 6 and 7) are XX, XX and XX respectively.

4.3 Effect of Clearance Ratio of Twisted Tape

Clearance of the twisted tape inserts has been varied inside the tube and its effects has been studied on outlet temperature, warmth relocate speed and pressure drop for different mass flow rates at the tube inlet. We take the three different twisted tapes of different values of the clearance ratios (c/D) = 0.166, 0.272 and 0.4 and with twist ratio of 5 in order to study its effects on warmth relocate speed, pressure drop and outlet temperature for all the mass flow rates ($\dot{m}$ = XX gm/s, XX gm/s and XX gm/s) with the help of commercial CFD (Computational Fluid Dynamics) algorithm, ANSYS FLUENT.

The curve between mass flow rates and the pressure drop are shown in Figure 4.5 for the different clearance ratios (c/D) = 0.166, 0.272 and 0.4 and with twist ratio of 5. It can be seen from the graph, as the clearance has increase, the pressure drop is decreased for all the inlet mass flow rates and this variation shows the good agreement with the literature review. This is due to fact that with increase in clearance ratio of the twisted tape, the less restriction is offered by the twisted tape to the swirl motion of the flow which leads to decrease in the pressure drop. Turbulence causes enhanced fluid assimilation between nearly wall section and central section at the expense of an increased pressure drop so, heat transfer in tubes can be improved by fluid assimilation without the need of any external power source.

It can be seen from the graph, as the clearance ratios (c/D) = 0.166, 0.272 and 0.4 has increase, pressure drop is decreased for all the tube inlet mass flow rates ($\dot{m}$ = XX gm/s, XX gm/s and XX gm/s) and this is due to the fact that with increase in the clearance ratios (c/D) = 0.166, 0.272 and 0.4) of twisted tape, the swirl motion in the flow goes down which leads to decrease in the pressure drop. Turbulence causes enhanced fluid assimilation between nearly wall section and central section at the expense of an increased pressure drop. It can be seen from the graph, as the clearance has increase, the pressure drop is decreased for all the inlet mass flow rates and this variation shows the good agreement with the literature review.

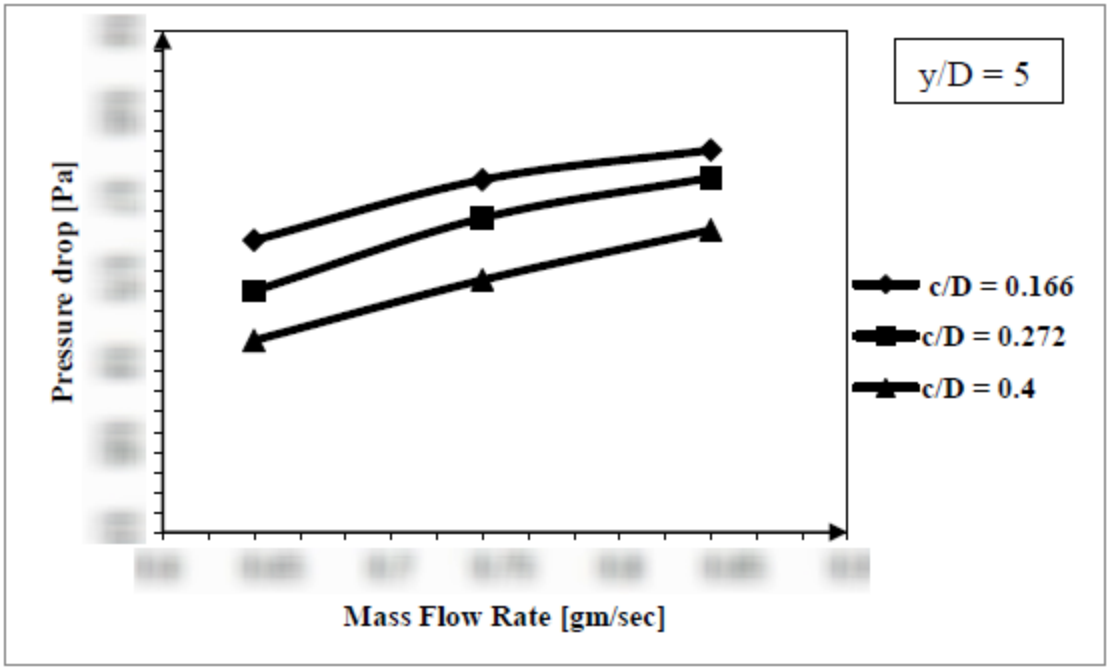

Figure 4.5: Pressure drop versus mass flow rate for different clearance ratios

Figure 4.6 shows variation warmth relocate speed for the tube with twisted tapes of different clearance values. Clearance of the twisted tape turbulators has been varied inside tube and its effects has been studied on heat transfer rate for different tube inlet mass flow (ṁ = XX gm/s, XX gm/s and XX gm/s). We take the three different twisted tapes of different values of the clearance ratios (c/D) = 0.166, 0.272 and 0.4 and with twist ratio of 5 in order to study its effects on the heat transfer rate with the help of commercial CFD (Computational Fluid Dynamics) algorithm, ANSYS FLUENT.

The curve between the mass flow rates and the heat transfer rate are shown in Figure 4.6 for the different clearance ratios (c/D) = 0.166, 0.272 and 0.4 and with twist ratio of 5. It can be seen from the graph, as the clearance has increase, warmth relocate speed decreases for all tube inlet mass flow rates flow (ṁ = XX gm/s, XX gm/s and XX gm/s) and this variation shows the good conformity with the literature review. From results we found that as we increase the tube inlet mass flow rate, heat transfer rate and pressure drop values are also increases. We found that with the increase of the clearance ratio from 0.166 to 0.4, heat transfer rate and pressure drop decreases for all tube inlet mass flow rates flow (ṁ = XX gm/s, XX gm/s and XX gm/s). It can be seen from the graph, as the clearance has increase, warmth relocate speed decreases for all tube inlet mass flow rates flow and this variation shows the good conformity with the literature review.

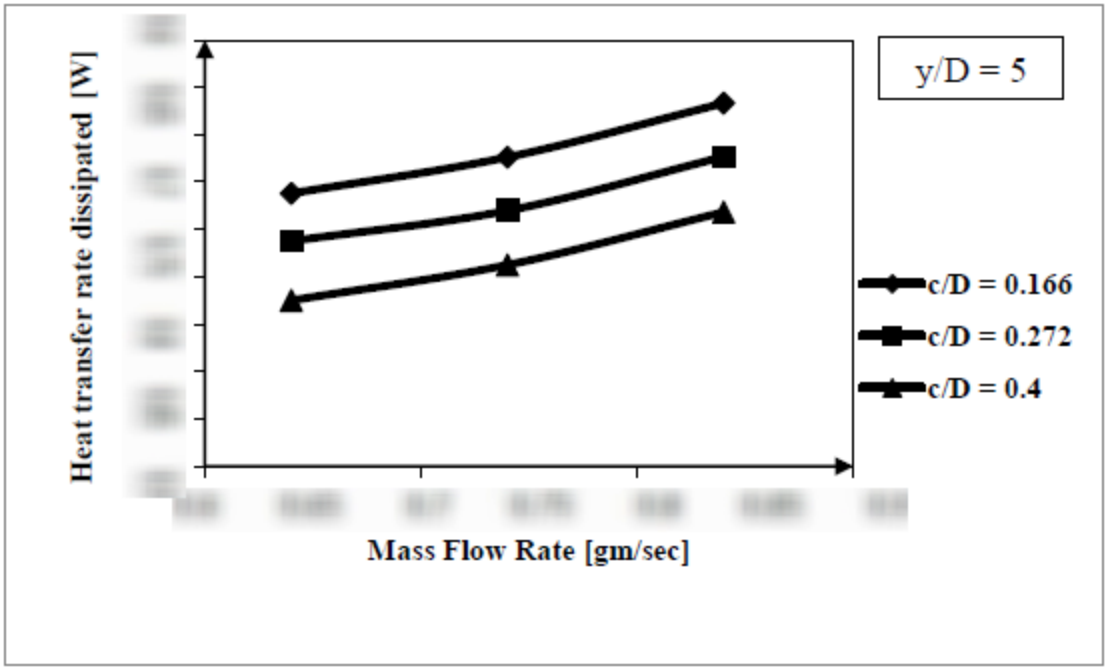

Figure 4.6: Heat transfer rate dissipated versus mass flow rate for different clearance ratios

The heat transfer rate in tube with twisted tape with different clearance ratios (c/D = 0.166, 0.272 and 0.4) are 1.32, 1.22 and 1.12 times respectively of those in the simple tube and pressure drop value in tube with twisted tape of different clearance ratios (c/D = 0.166, 0.272 and 0.4) are 2.85, 2.77 and 2.19 times respectively of those in the plain tube of XX mm diameter. The thermal performance improvement for the different clearance ratios (c/D = 0.166, 0.272 and 0.4) are XX, XX and XX respectively as compare to the plain tube of XX mm diameter.

4.4 Comparison of different designs

Eight designs were compared with the actual design by keeping all the parameters and boundary conditions fixed other than making geometrical changes. Figure 4.7 shows the outlet temperatures obtained for different designs.

4.4.1 Temperature variation at the tube outlet

It can be seen from Figure 4.7 that the outlet temperatures for mass flow rate of XX gm/s are approximately same for all the designs because the PJA is immersed in water all the time and the surrounding water temperature inside the tray drip is XX^{o}C and the saturation temperature of the refrigerant (iso-butane) is also XX^{o}C. We take single phase flow for our simulation so the minimum temperature which can be obtained at the outlet would be XX^{o}C. As we can be seen from the Figure 4.7, we compared the outlet temperatures of all the designs of PJA tube with and

without putting twisted tape of dissimilar twist ratio and clearance ratio inside the tube. It can be seen from the results that the minimum outlet temperature is obtained in case of tube with the twisted tape with twist ratio of 5 and as we increase twist ratio and clearance ratio, outlet temperature also get increased. The outlet temperature difference between all the designs is very less. The maximum outlet temperature is obtained in case of tube with XX mm diameter without the twisted tape inserts.

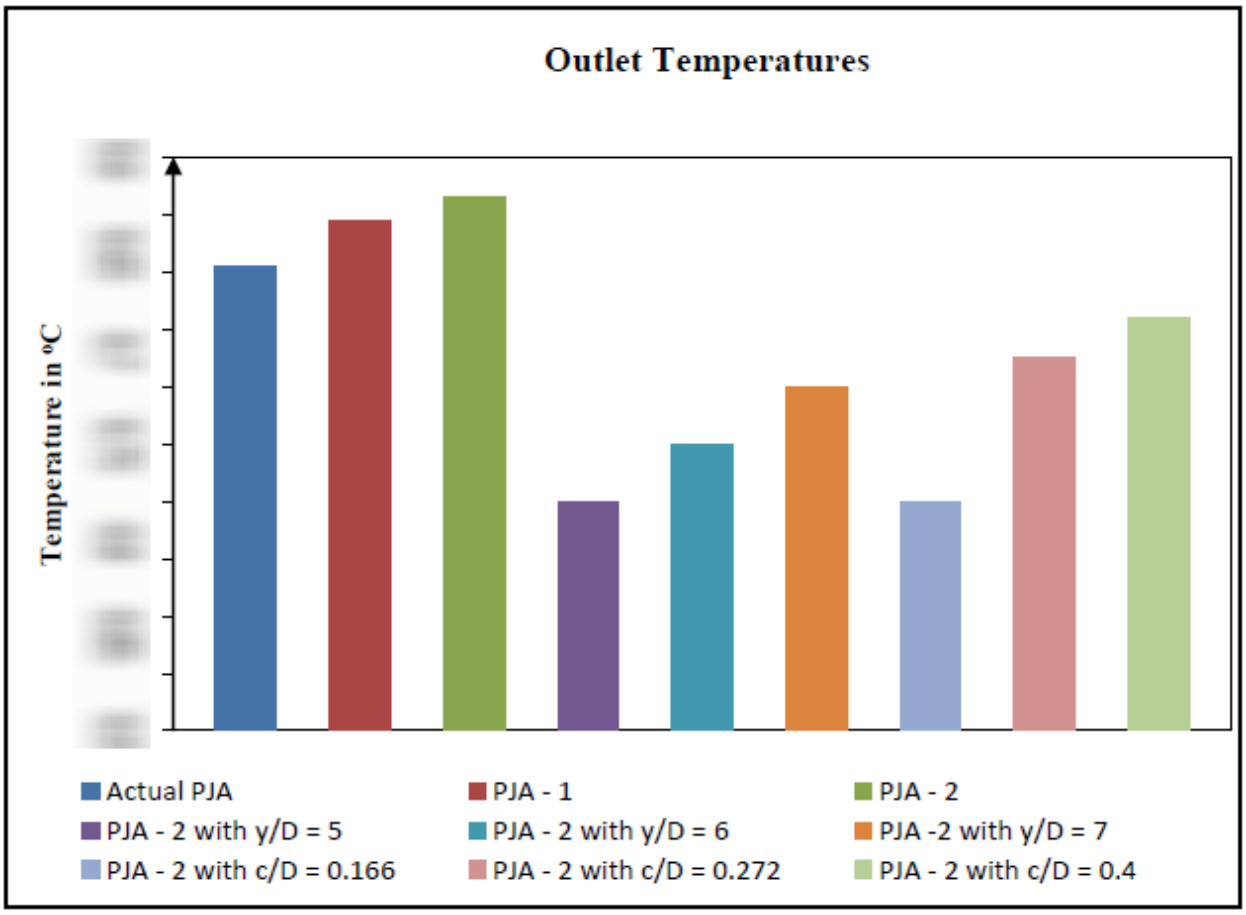

Figure 4.7: Outlet temperatures for different designs

As we can be seen from the Figure 4.7, we take twisted tape inserts of three different twist ratios (y/D) = 5, 6 and 7 and three different clearance ratios (c/D) = 0.166, 0.272 and 0.4. From results we can observe that the minimum outlet temperature is received in the case of tube with twisted tape of minimum twist ratio of 5 and minimum clearance ratio of 0.166 and as we increase the twist ratio of the clearance ratio of twisted tape turbulators, the outlet temperature increases.

4.4.2 Temperature variation at the cross-section of the tube

Variation of temperature has been plotted at one of the cross-section of the tube which is at a distance of XX mm from the tube inlet. To explain the difference between the results caused by the occupied piece twisted tapes of different twist ratios, we take mass flow rate (ṁ) = XX gm/s as an example and present the plots of temperature variations.

4.4.2.1 Temperature variation at the cross-section of plane tube

To plot the variation of temperature, we consider two axis x-axis and y-axis at the center of the cross-section as shown in the Figure 4.8.

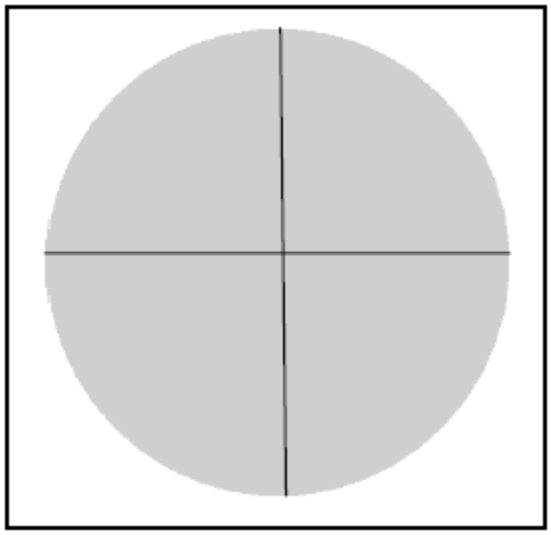

Figure 4.8: Cross-section plane of tube with both axes

Variation of temperature along x-axis and y-axis has been plotted for the mass flow rate (ṁ) = XX g/s on the cross-section as we can see in Figures 4.9 and 4.10 respectively. From the results it is observe that temperature of the fluid is minimum near walls and maximum at center of tube. The maximum temperature at the center of tube is around XX^{o}C which is nearly equal to the inlet temperature of fluid and minimum temperature of fluid near wall is around XX^{o}C which is equal to the outside water temperature around the tube in the tray drip. For both the axes, the variation of temperature against the distance is around same. From the results it is observe that temperature of the fluid is minimum near walls and maximum at center of tube. The maximum temperature at the center of tube is around XX^{o}C which is nearly equal to the inlet temperature of fluid and minimum temperature of fluid near wall.

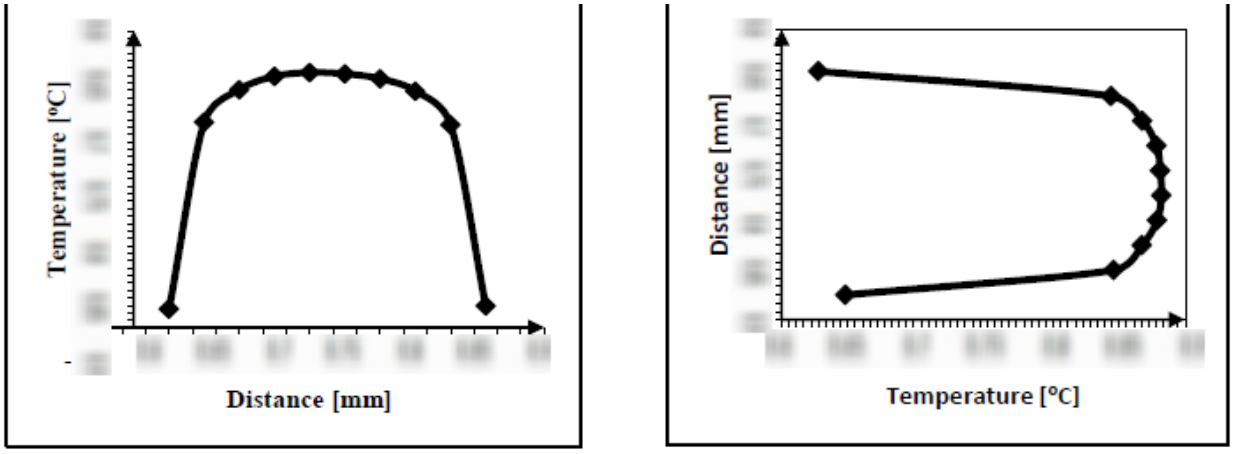

Figure 4.9: Variation of temperature along x-axis and y-axis

4.4.2.2 Temperature variation at the cross-section of tube with TT turbulators

Turbulence causes enhanced fluid assimilation amid nearly wall region and central region at expense of an increased pressure drop so, heat transfer in tubes can be improved by fluid assimilation without the need of any external power source. To plot the variation of temperature for the twisted tape turbulators of three different twist ratios (y/D) = 5, 6 and 7 and three dissimilar clearance ratios (c/D) = 0.166, 0.272 and 0.4, we consider x-axis at the center of the cross-section as shown in the Figure 4.10.

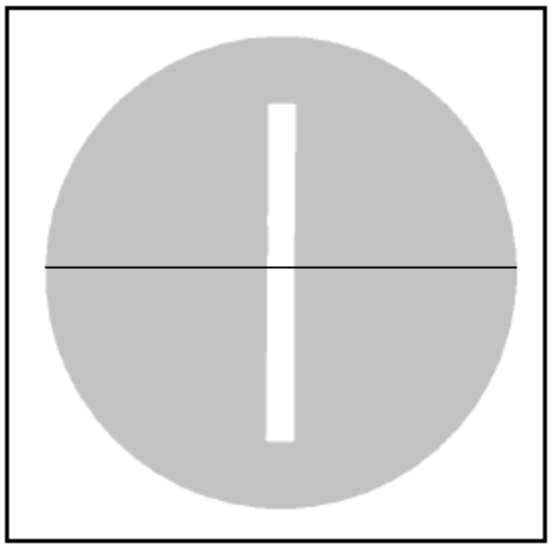

Figure 4.10: Cross-section plane of tube with TT with x-axis

a) For tube with TT of twist ratio 5

From the results it is observe that temperature of the fluid is minimum near the walls and maximum around the center of tube with twisted tape turbulator of twist ratio 5 and clearance ratio 0.166. The maximum temperature around the center of tube is around XX^{o}C which is nearly equal to the inlet temperature of fluid and the minimum temperature of fluid near wall is around XX^{o}C. From the Figure 4.12, it is observe that at a distance of 0.6 mm from the tube wall, the temperature of the fluid is around XX^{o}C. At a distance of 1.2 mm from the wall, the temperature of the fluid becomes maximum.

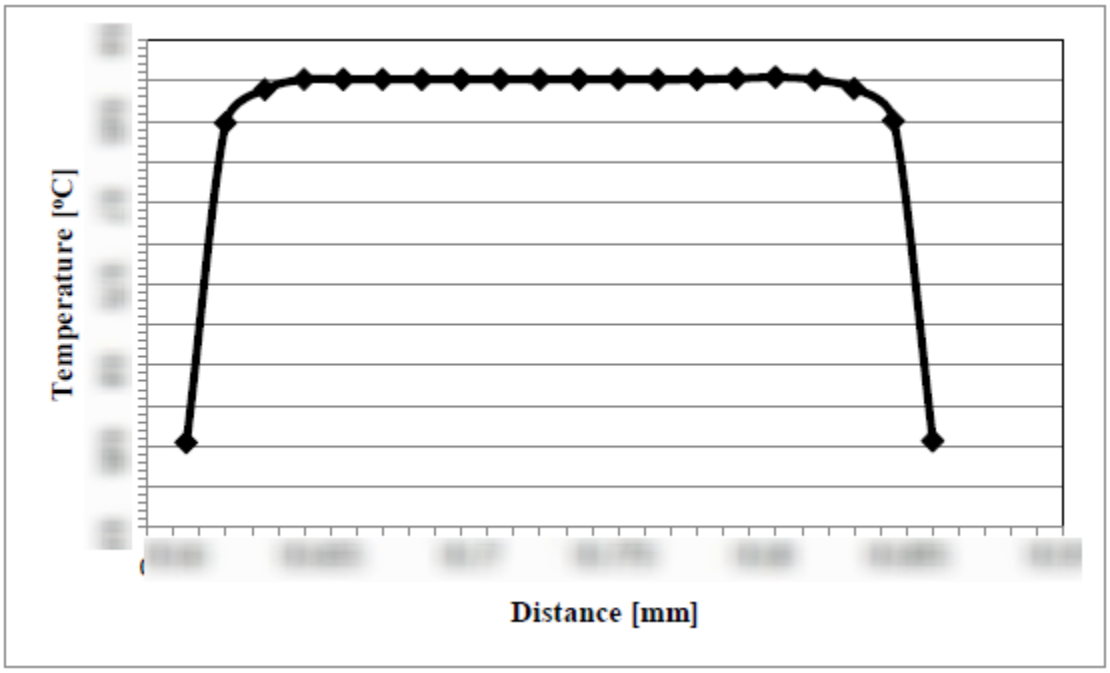

Figure 4.11: Variation of temperature for tube with TT of TR 5 along x-axis

b) For tube with TT of twist ratio 6

For tube with twisted tape of twist ratio 6 and clearance ratio 0.166 it is observe that temperature of the fluid is minimum near walls and maximum around center of tube. The maximum temperature around the center of tube is around XX^{o}C which is nearly equal to the inlet temperature of fluid and minimum temperature of fluid near the wall is around XX^{o}C. From the Figure 4.13, it is observe that at a distance of 0.6 mm from the tube wall, the temperature of the fluid is around XX^{o}C. At a distance of 2.1 mm from the wall, the temperature of the fluid becomes maximum.

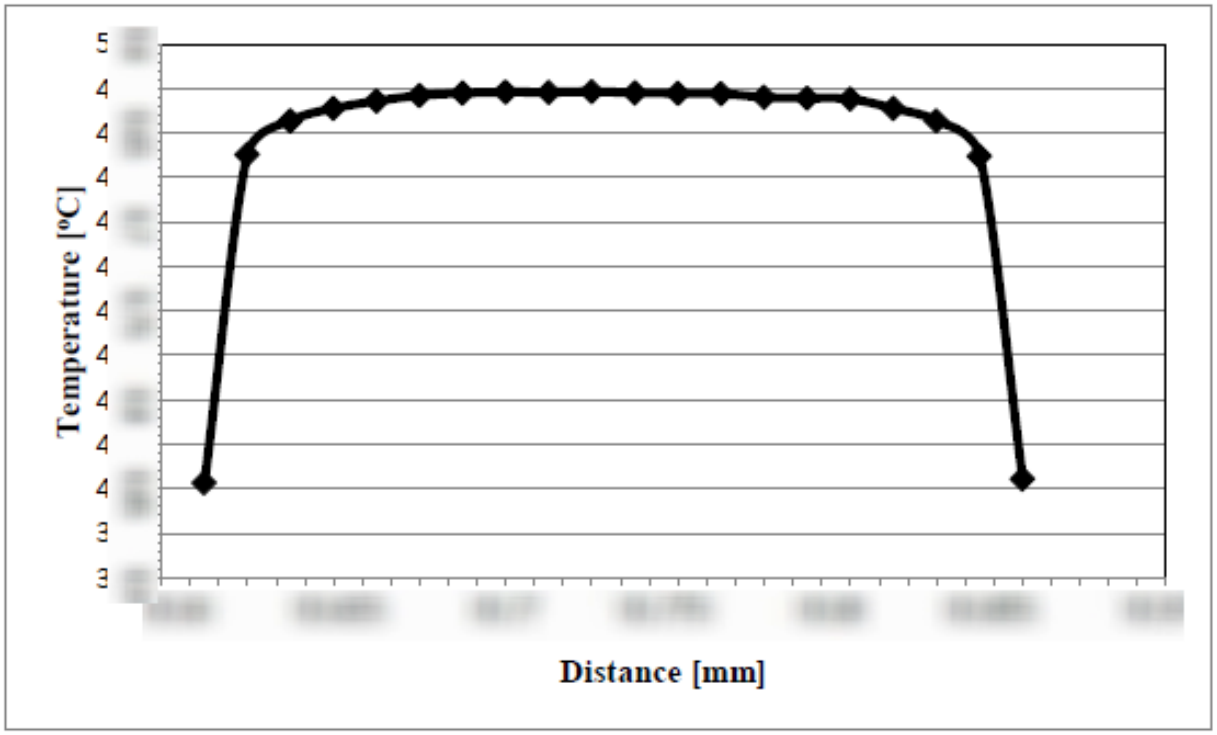

Figure 4.12: Variation of temperature for tube with TT of TR 6 along x-axis

c) **For tube with TT of twist ratio 7**

The Turbulence causes enhanced fluid assimilation between nearly wall section and the central section at expense of an increased pressure drop so, heat transfer in tubes can be improved by fluid mixing without the need of any external power source. To plot the variation of temperature for the twisted tape turbulators of twist ratio (y/D) = 7 and three different clearance ratio (c/D) = 0.166, we consider x-axis at center of the cross-section as shown in the Figure 4.13.

From the results it is observe that temperature of the fluid is minimum near walls and maximum around center of tube with twisted tape insert of twist ratio 7 and clearance ratio 0.166. The maximum temperature around the center of tube is around XXºC which is nearly equal to the inlet temperature of fluid and minimum temperature of fluid near the wall is around XXºC. From the Figure 4.13, it is observe that at a distance of 0.6 mm from the tube wall, the temperature of the fluid is around XXºC. At a distance of 2.4 mm from the wall, the temperature of the fluid becomes maximum.

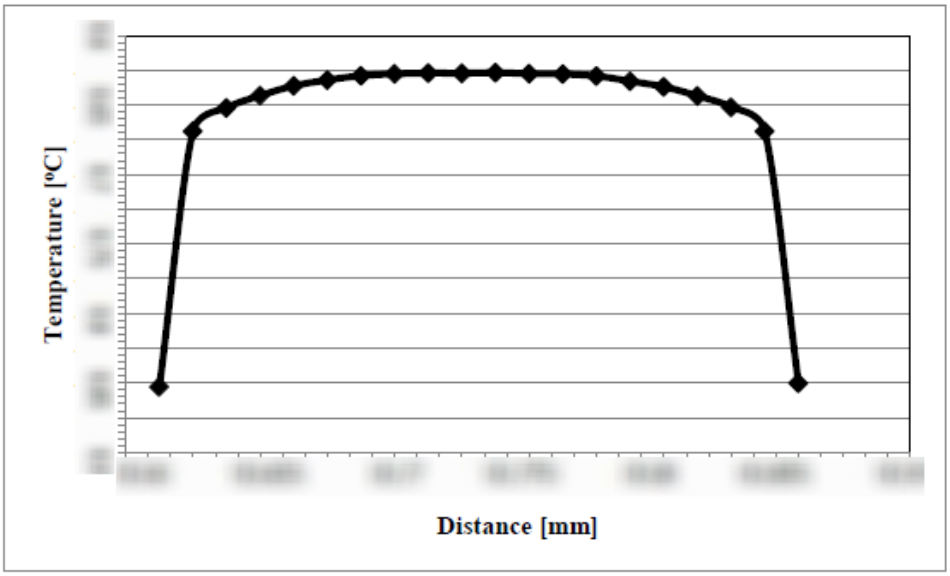

Figure 4.13: Variation of temperature for tube with TT of TR 7 along x-axis

4.4.3 Velocity variation at cross-section of tube

Variation of velocity has been plotted at one of the cross-section of the tube which is at a distance of XX mm from the tube inlet. To explain the difference between the results caused by the full length twisted tapes of dissimilar twist ratios, we take mass flow rate (ṁ) = XX gm/s as an example and present plots of temperature variations.

4.4.3.1 Velocity variation at the cross-section of plain tube

To plot the variation of velocity, we consider x-axis at the center of the cross-section as shown in the Figure 4.14.

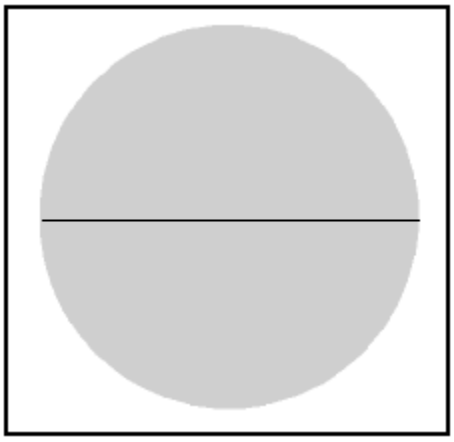

Figure 4.14: Cross-section plane of tube with x-axis

Variation of velocity along x-axis has been plotted for the mass flow rate (ṁ) = XX g/s on the cross-section as shown in Figure 4.15. From the results it is observe that velocity of the fluid is minimum near the walls due to the wall friction and no slip condition and maximum at the center of the tube. The maximum velocity at center of tube is around 1.4 m/s which is nearly equal to inlet velocity of fluid and minimum velocity of fluid near the wall is around 0.1 m/s.

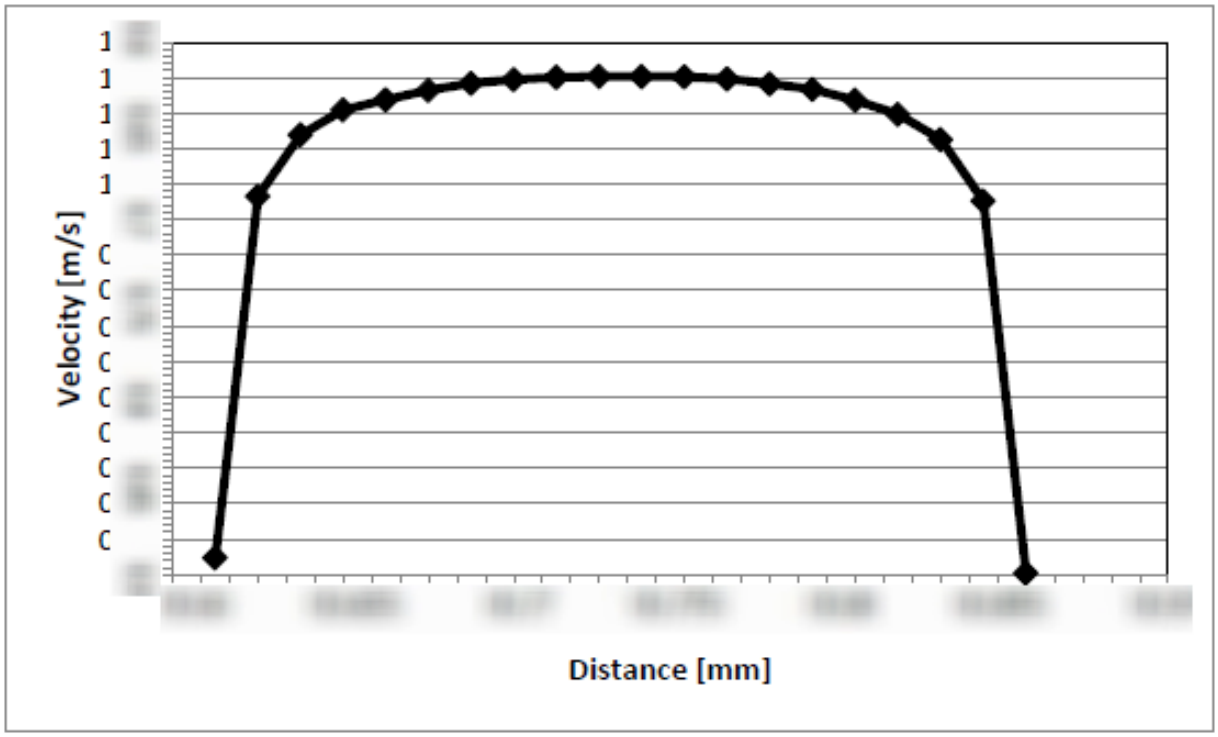

Figure 4.15: Variation of velocity w.r.t to x-axis

4.4.3.2 Velocity variation at the cross-section of tube with TT turbulators

Turbulence causes enhanced fluid assimilation between nearly wall section and the central section at expense of an increased pressure drop so, the heat transfer in tubes can be improved by fluid assimilation and producing swirl flow without the need of any external power source.

To plot the variation of temperature, we consider x-axis at center of the cross-section as shown in Figure 4.16. Variation of temperature has been plotted for different twist ratios and clearance ratios.

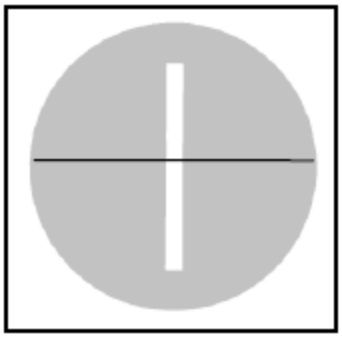

Figure 4.16: Cross-section plane of tube with TT with x-axis

From the results it is observe that velocity of the fluid is minimum near tube wall and near wall of twisted tape and maximum around center of the distance between tube and twisted tape insert. The maximum velocity is around 1.5 m/s on both the sides of the tape as shown in the Figure 4.17 and the fluid has no velocity near the walls.

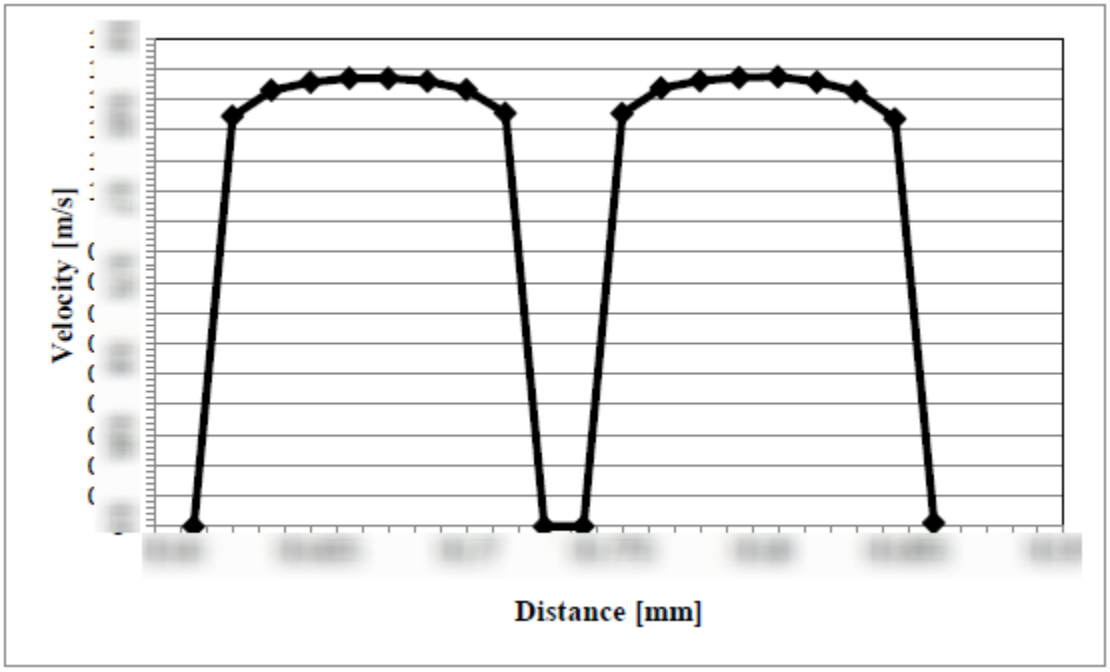

Figure 4.17: Variation of velocity for tube with TT along x-axis

4.5 Pressure and temperature distributions

4.5.1 Pressure distribution for actual design of PJA

Pressure of the superheated refrigerant vapors is higher at the inlet and decreases as it moves towards outlet as shown in Figure 4.18. The high pressure gradient along the tube is due to the

friction between refrigerant and tube wall and also due to the bending loses. The pressure drop across the PJA is around XX Pa.

4.5.2 Pressure distribution for PJA-1

As we increase the diameter of the tube from XX mm to XX mm by keeping the same surface area and the length of the tube reduce from XX mm to XX mm. Due to the increase the diameter of tube and decrease length of tube we get very low pressure drop in this case as compare to the actual design of the PJA. In this case the pressure drop gets reduced from XX Pa to XX Pa due to which the pumping power also gets reduced from XX Watt to XX Watt. The pressure drop across the PJA is around XX Pa.

4.5.3 Pressure distribution for PJA-2

We further increase the diameter of the tube from XX mm to XX mm by keeping the same surface area and the length of the tube is reduced from XX mm to XX mm in order to get the more benefit over pressure drop. In this case pressure drop get reduced from the XX Pa to XX Pa due to which the pumping power get also reduced from XX Watt to XX Watt. If we compare this design to the actual model of the PJA which is presently using by LG then we observe that the pressure drop is reduced from XX Pa to XX Pa and pumping power is reduced from XX Watt to XX Watt without compromising the total heat transfer rate and total surface heat flux. This PJA design has very huge advantage over the presently using PJA design in terms of pressure drop and pumping power which further increase the energy efficiency of the refrigerator. As this design gives us the maximum thermal performance improvement so we choose the design of PJA with XX mm diameter. The pressure drop across the PJA is around XX Pa.

4.5.4 Pressure distribution for PJA-2 with TT turbulators

To increase total heat transfer rate of PJA-2 we place the twisted tape of different twist ratios and with dissimilar clearance inside tube. From the consequences we observe that by using the twisted tape inside the tape the pressure drop as well as total heat transfer rate increases. By using twisted tape of twist ratio 5, the pressure drop increases from XX Pa to XX Pa and heat transfer rate increases from XX Watt to XX Watt and with the twist ratio 6, the pressure drop increases from XX Pa to XX Pa and heat transfer rate increases from XX Watt to XX Watt and by using the twisted tape of twist ratio 7, the pressure drop increases from XX Pa to XX Pa and the heat transfer rate increases from XX Watt to XX Watt. From results we observe that as we

increase the twist ratio of the tube from 5 to 7, the pressure drop reduces from XX Pa to XX Pa and heat transfer rate reduces from XX Watt to XX Watt.

4.5.5 Temperature distribution for actual design of PJA

Results shows that the temperature distribution of PJA heat exchanger along its length. The temperature plot reveals that the superheated refrigerant vapor loses heat to the defrost water as it moves through the pipe. At the outlet, the temperature of the refrigerant vapor becomes equal to the water temperature (XX^{o}C) which is placed inside the tray drip and its saturated temperature also XX^{o}C. The temperature of the refrigerant vapor does not go below XX^{o}C. Only half of the length of the PJA is utilized to drop the temperature of the refrigerant vapor from XX^{o}C to XX^{o}C and other half of the length have no use in the heat transfer process. So this simulation will be helpful to us in order to reduce the cost of the PJA by reducing its non effective length which does not take part in heat transfer process. The temperature drop of superheated refrigerant vapor is around XX^{o}C.

4.5.6 Temperature distribution for PJA-1

As we increase the diameter of the tube from XX mm to XX mm by keeping the same surface area and the length of the tube reduce from XX mm to XX mm. Due to the increase the diameter of tube and decrease length of tube we get very less increment in the outlet temperature in this case as compare to the actual design of the PJA. In this case the pressure drop gets reduced from XX Pa to XX Pa due to which the pumping power also gets reduced from XX Watt to XX Watt. So in this case we get same temperature difference with the benefit over the pressure drop. In this case the superheated refrigerant vapor coming out from the compressor at XX^{o}C temperature passes through the PJA tube which is placed inside the tray drip. In the tray drip the water is present at XX^{o}C temperature which cools down the superheated refrigerant vapor up to its saturation temperature (XX^{o}C) as it passes through the PJA tube. So the temperature drop of superheated refrigerant vapor is around XX^{o}C.

4.5.7 Temperature distribution for PJA-2

In this case due to the increase in the diameter of the tube from XX mm to XX mm by keeping the same surface area and the length of the tube reduce from XX mm to XX mm. Due to the increase the diameter of tube and decrease length of tube we get very less increment in the outlet temperature in this case as compare to the actual design of the PJA. In this case the pressure drop

gets reduced from XX Pa to XX Pa due to which the pumping power also gets reduced from XX Watt to XX Watt. So in this case we get same temperature difference with the benefit over the pressure drop. In this case the superheated refrigerant vapor coming out from the compressor at XX^{o}C temperature passes through the PJA tube which is placed inside the tray drip. In the tray drip the water is present at XX^{o}C temperature which cools down the superheated refrigerant vapor up to its saturation temperature (XX^{o}C) as it passes through the PJA tube. So the temperature drop of superheated refrigerant vapor is around XX^{o}C.

4.5.8 Temperature distribution for PJA-2 with TT turbulators

In this case, to augment total heat transfer rate of PJA-2 we place the twisted tape of different twist ratios and with different clearance inside tube. From the consequences we observe that by using the twisted tape inside the tape the pressure drop as well as total heat transfer rate increases. By using the twisted tape of twist ratio 5, the heat transfer rate increases from XX Watt to XX Watt and with the twist ratio 6, the heat transfer rate increases from XX Watt to XX Watt and by using the twisted tape of twist ratio 7, the heat transfer rate increases from XX Watt to XX Watt. From results we observe that as we increase the twist ratio of the tube from 5 to 7, the heat transfer rate reduces from XX Watt to XX Watt. Clearance ratios of the twisted tape inside tube also affect heat transfer rate inside the tube. By using twisted tape of clearance ratios 0.166, 0.272 and 0.4, the heat transfer rate decreases from XX Watt to XX Watt. From the results we can observe that as we increase the clearance ratio of the twisted tape inside tube, heat transfer rate inside the tube decreases.

4.6 Velocity and temperature distribution for TT of different widths

To explain the difference between the results caused by the full length twisted tapes of different widths, we take mass flow rate ($\dot{m}$) = XX gm/s as an example and present plots velocity contours, temperature contours and tangential velocity vector of the same location at distance (d) = XX mm from the inlet of the tube.

4.6.1 Velocity Distribution for TT of different widths

The velocity contours at the cross-section plane at length of XX mm from inlet for the plain tube. Due to the wall resistance and due to the no slip condition at the wall, the velocity boundary layer is formed near the wall due to which the velocity of the fluids layers near the wall is relatively very small as compare to the fluid layers at the centre of the tube. These boundary

layers or laminar sub a layer behaves like an insulator and restrict the heat transfer between the fluid and the tube wall due to which the effectiveness of the heat exchanger reduces. In order to break that layer, the twisted tape turbulators inserted inside the tube which produces the swirl motion of the fluid inside the tube and increases the turbulence inside the tube due to which the thickness of the boundary layer also get reduced. As shown in the Figures 4.28, 4.29 and 4.30, twisted tape of different width (D = XX mm, XX mm and XX mm) is inserted inside the tube. From the results we observe that as we insert the twisted tape inside the tube, the velocity of the fluid is increases and we get maximum velocity of XX m/s in case of tube with twisted tape of width (D= XX mm) and as we decrease the width of the tape, the velocity of the fluid also decreases and the boundary layer thickness increases.

4.6.2 Temperature distribution for TT of different widths

It demonstrate that, the thermal boundary layer thickness is much higher in case of plain tube as compare to the tube with the twisted tapes and results also demonstrate that as the width of the tape decreases, the thermal boundary layer grows thicker which behaves like an insulator and restrict the heat transfer between wall and fluid. Twisted tape inserts disturb the boundary layer formation and enhances the heat transfer rate inside the tube.

4.7 Comparison of actual and final design

From the results of heat transfer rate and pressure drop variation it has been found that with the increase in the diameter of tube by keeping the same surface area, the pressure drop reduces drastically without compromising the total heat transfer rate. Also, by comparing the different designs it is observed that the addition of twisted tape inserts inside the tube increases the heat transfer rate. Hence, both of these effects are combined to obtain the final model which was operated with the tube of XX mm diameter with twisted tape inserts of twist ratio 5 and clearance ratio 0.166 with mass flow rate of XX gm/s. The result obtained from final model is compared with the actual model.

Figure 4.18 shows the comparison of pressure drop between actual and final design of the PJA (Pipe Joint Assembly). It can be seen from the graph that there is very less pressure drop of the refrigerant vapor in the final model as compare to the actual model. This is because of increases of the diameter from XX mm to XX mm and decreases of the length of the tube from XX mm to XX mm which reduces the flow friction and leads to decrease the pressure drop from XX to XX

Pa. It is found that with increase in the diameter of the tube from XX mm to XX mm and decrease the length of the tube from XX mm to XX mm in order to keep the surface area same i.e. XX m^2, the pressure drop reduces from XX Pa to XX Pa and outlet temperature of refrigerant vapor and the total heat transfer rate remains same. So tube with XX mm diameter with twisted tape turbulators found optimum for the operation of heat exchanger.

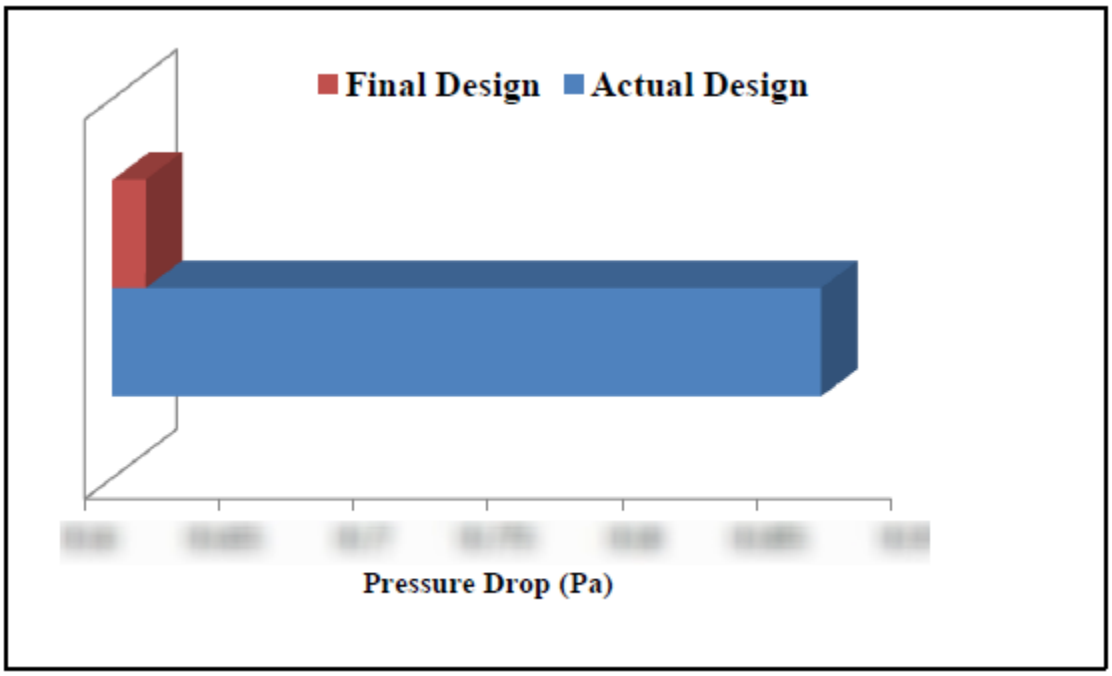

Figure 4.18: Comparison of pressure drop between actual and final design

Figure 4.19 shows the comparison of the heat transfer rate between the actual and final design of the PJA (Pipe Joint Assembly). It can be seen from the figure that there is increase in the heat transfer rate in final design as compare to the actual design. This is because of the presence of the twisted tape inside the tube which increases the turbulence inside the tube due to which further leads to increase heat transfer rate from XX to XX Watt. We choose the twisted tape of twist ratio 5 and clearance ratio 0.166 as it gives us the maximum amount of heat transfer as compare to the others.

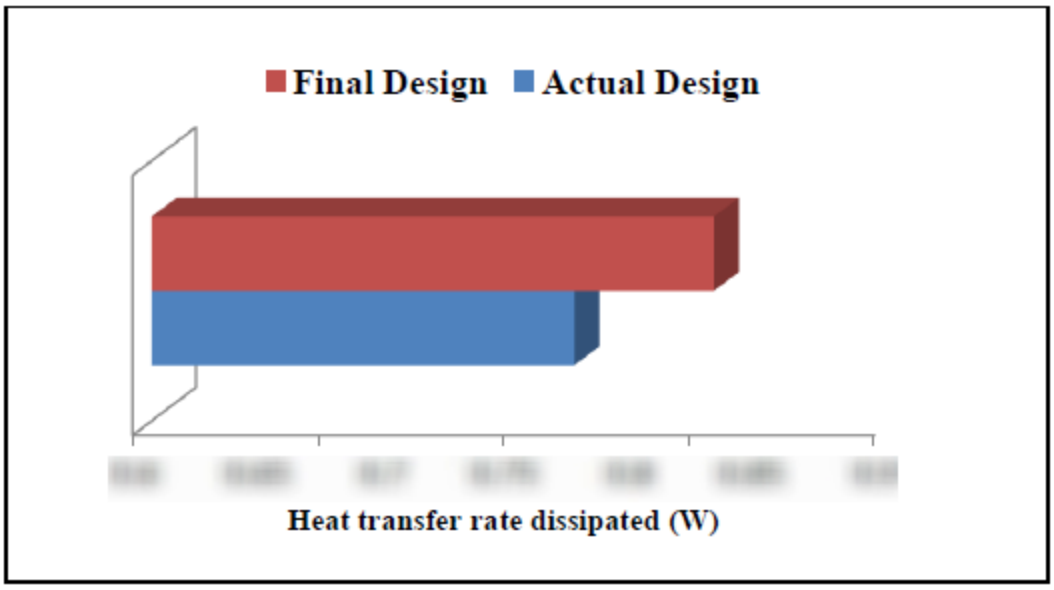

Figure 4.19: Comparison of heat transfer rate between actual and final design

Figure 4.20 shows the comparison of the outlet temperature between the actual and final design of the PJA (Pipe Joint Assembly). It can be seen from the figure that there is slight decrease in the outlet temperature in final design as compare to the actual design. This is because of the presence of the twisted tape inside the tube which increases the turbulence inside the tube.

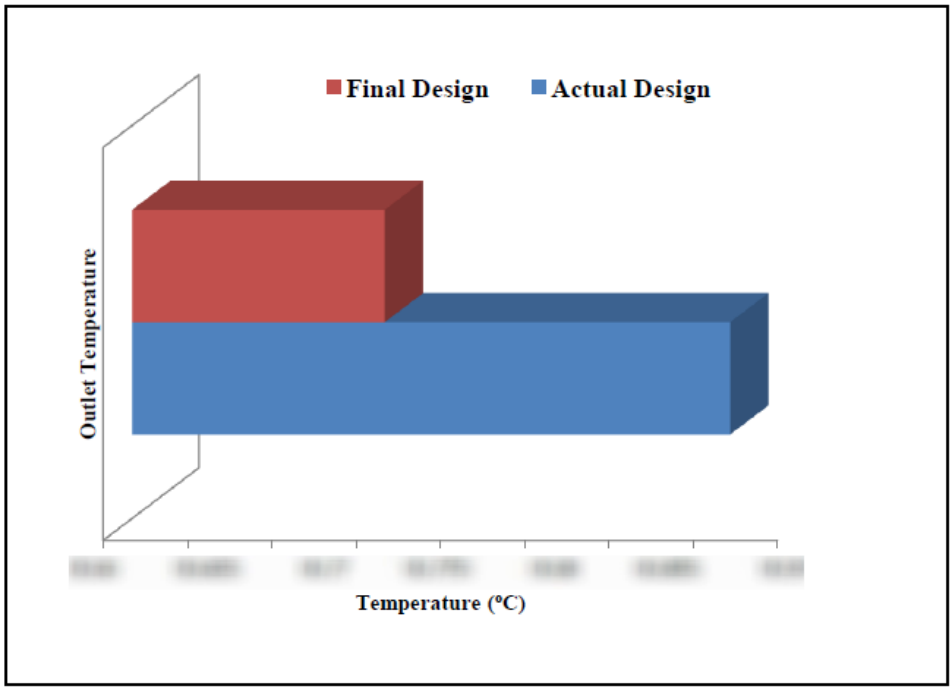

Figure 4.20: Comparison of outlet temperature between actual and final design

Chapter 5 : CONCLUSION

The CFD simulation of the pipe joint assembly (PJA) has been performed and the following conclusions were made.

- It is found that with increase in the diameter of the tube from XX mm to XX mm and decrease the length of the tube from XX mm to XX mm in order to keep the surface area same i.e. XX m2, the pressure drop reduces from XX Pa to XX Pa and outlet temperature of refrigerant vapor and the total heat transfer rate remains same. So tube with XX mm diameter found optimum for the operation of heat exchanger.

- The maximum increase of 26% has been obtained in the total heat transfer rate dissipated, whereas an increase of 58% is observed in the pressure drop, when the mass flow rate was increased from XX gm/s to XX gm/s at the inlet of the tube of XX mm diameter.

- Results obtained from the CFD simulation have shown close agreement with the theoretical results for different inlet mass flow rates.

- The addition of twisted tape inside the tube has resulted in decrease in outlet temperatures of the hot refrigerant vapor and increase in the pressure drop and heat transfer rate inside the tube. This is due to the increase in turbulence inside the tube due to the swirl flow of the refrigerant vapor.

- From the results it has been observed that as we increase the twist ratio of the twisted tape from 5 to 7 by keeping the same clearance ratio of 0.166, the heat transfer rate decreases from XX Watt to XX Watt and the pressure drop decreases from XX Pa to XX Pa. So twisted tape with twist ratio 5 found optimum for the operation of heat exchanger because we get more heat transfer rate in this case as compare to the others.

- From the simulation results it has been observed that as we increase the clearance ratio of the twisted tape from 0.166 to 0.4 by keeping the same twist ratio of 5, the heat transfer rate decreases from XX Watt to XX Watt and the pressure drop decreases from XX Pa to XX Pa. So twisted tape with clearance ratio 0.166 found optimum for the operation of heat exchanger because we get more heat transfer in this case as compare to others.

- A final design of tube with twisted tape inserts of twist ratio 5 and clearance ratio 0.166 with inlet mass flow rate of XX gm/s was found to give better heat results than the actual design with even lesser pressure drop. An increase of 32% is observed in the heat transfer rate and decrease of pressure drop from XX to XX is observed with proposed design in comparison to the actual design.

FUTURE SCOPE OF WORK

The use of Pipe Joint Assembly (PJA) in the Free Frost refrigerator is a growing technology and there are many areas in which further work can be carried out:

1) Modification in the other geometrical parameters such as number of bends and surface roughness, surface with dimples can also further improve the heat transfer rate.

2) Additional cuts on the surface of the twisted tape can be used to make the flow more turbulent.

3) Analytical techniques can also be employed to investigate pressure and temperature distribution.

4) In the present study, effect of changing the thickness of the tape is not studied. So in future, effect of the thickness of tape on the stream line, velocity distribution, pressure distribution and on the heat transfer rate can be computed.\

5) For the same set of turbulators, heat transfer and friction characteristics can be studied for laminar flow condition.

REFRENCES

1) Hejazi, V., Akhavan-Behabadi, M. and Afshari, A. (2010). Experimental investigation of twisted tape inserts performance on condensation heat transfer enhancement and pressure drop. *International Communications in Heat and Mass Transfer*, 37(9), pp.1376-1387.

2) Bas, H. and Ozceyhan, V. (2012). Heat transfer enhancement in a tube with twisted tape inserts placed separately from the tube wall. *Experimental Thermal and Fluid Science*, 41, pp.51-58.

3) Eiamsa-ard, S., Thianpong, C., Eiamsa-ard, P. and Promvonge, P. (2009). Convective heat transfer in a circular tube with short-length twisted tape insert. *International Communications in Heat and Mass Transfer*, 36(4), pp.365-371.

4) Eiamsa-ard, S., Thianpong, C. and Promvonge, P. (2006). Experimental investigation of heat transfer and flow friction in a circular tube fitted with regularly spaced twisted tape elements. *International Communications in Heat and Mass Transfer*, 33(10), pp.1225-1233.

5) He, Y., Liu, L., Li, P. and Ma, L. (2018). Experimental study on heat transfer enhancement characteristics of tube with cross hollow twisted tape inserts. *Applied Thermal Engineering*, 131, pp.743-749.

6) Piriyarungrod, N., Kumar, M., Thianpong, C., Pimsarn, M., Chuwattanakul, V. and Eiamsa-ard, S. (2018). Intensification of thermo-hydraulic performance in heat exchanger tube inserted with multiple twisted-tapes. *Applied Thermal Engineering*, 136, pp.516-530.

7) Eiamsa-ard, S. and Promvonge, P. (2010). Performance assessment in a heat exchanger tube with alternate clockwise and counter-clockwise twisted-tape inserts. *International Journal of Heat and Mass Transfer*, 53(7-8), pp.1364-1372.

8) Li, P., Liu, Z., Liu, W. and Chen, G. (2015). Numerical study on heat transfer enhancement characteristics of tube inserted with centrally hollow narrow twisted tapes. *International Journal of Heat and Mass Transfer*, 88, pp.481-491.

9) Thianpong, C., Eiamsa-ard, P., Wongcharee, K. and Eiamsa-ard, S. (2009). Compound heat transfer enhancement of a dimpled tube with a twisted tape swirl generator. *International Communications in Heat and Mass Transfer*, 36(7), pp.698-704.

10) Hong, S. and Bergles, A. (1976). Augmentation of Laminar Flow Heat Transfer in Tubes by Means of Twisted-Tape Inserts. *Journal of Heat Transfer*, 98(2), p.251.
11) Promvonge, P. (2008). Thermal augmentation in circular tube with twisted tape and wire coil turbulators. *Energy Conversion and Management*, 49(11), pp.2949-2955.
12) Murugesan, P., Mayilsamy, K., Suresh, S. and Srinivasan, P. (2011). Heat transfer and pressure drop characteristics in a circular tube fitted with and without V-cut twisted tape insert. *International Communications in Heat and Mass Transfer*, 38(3), pp.329-334.
13) Al-Fahed, S., Chamra, L. and Chakroun, W. (1998). Pressure drop and heat transfer comparison for both microfin tube and twisted-tape inserts in laminar flow. *Experimental Thermal and Fluid Science*, 18(4), pp.323-333.
14) Bergman, T. and Incropera, F. (2011). *Fundamentals of heat and mass transfer*. Hoboken, NJ: Wiley.
15) Promvonge, P. (2009). Thermal augmentation in circular tube with twisted tape and wire coil turbulators. *Energy Conversion and Management*, 49(11), pp.2949-2955.
16) Bergman, T. and Incropera, F. (2011). *Fundamentals of heat and mass transfer*. Hoboken, NJ: Wiley.
17) Bejan, A. (1993). *Heat transfer*. New York: John Wiley & Sons.
18) Cengel, Y. (2008). *Introduction to thermodynamics and heat transfer*. Boston, Mass. [u.a.]: McGraw-Hill Higher Education.
19) Hong, S. and Bergles, A. (1976). Augmentation of Laminar Flow Heat Transfer in Tubes by Means of Twisted-Tape Inserts. *Journal of Heat Transfer*, 98(2), p.251.
20) Hollanders, H., Krause, E., Lions, . and llmann, W. (1980). *Computational fluid dynamics*. Washington: Hemisphere Pub. Corp.
21) White, F. (n.d.). *Fluid mechanics*.
22) Khurmi, R. and Gupta, J. (2001). *Textbook of refrigeration and air conditioning (in SI units)*. New Delhi: Eurasia.
23) Marchi, C., Suero, R. and Araki, L. (2009). The lid-driven square cavity flow: numerical solution with a 1024 x 1024 grid. *Journal of the Brazilian Society of Mechanical Sciences and Engineering*, 31(3).

24) Biswas, G., Breuer, M. and Durst, F. (2004). Backward-Facing Step Flows for Various Expansion Ratios at Low and Moderate Reynolds Numbers. *Journal of Fluids Engineering*, 126(3), p.362.

Thesis ME

ORIGINALITY REPORT

9%	4%	7%	%
SIMILARITY INDEX	INTERNET SOURCES	PUBLICATIONS	STUDENT PAPERS

PRIMARY SOURCES

1	www.ideals.illinois.edu Internet Source	1%
2	www.nitkkr.ac.in Internet Source	1%
3	Halit Bas, Veysel Ozceyhan. "Heat transfer enhancement in a tube with twisted tape inserts placed separately from the tube wall", Experimental Thermal and Fluid Science, 2012 Publication	1%
4	www.ijmer.com Internet Source	1%
5	Piriyarungroj, Niwat, Smith Eiamsa-ard, Pongjet Promvonge, Petpices Eiamsa-Ard, and Chinaruk Thianpong. "Simulation of Turbulent Heat Transfer in a Tube Fitted with Twisted Tape Placed Separately from the Tube Walls", Applied Mechanics and Materials, 2015. Publication	<1%
6	N. Piriyarungrod, Manoj Kumar, C. Thianpong, M. Pimsarn, V. Chuwattabakul, S. Eiamsa-ard.	<1%